

*Exxon Valdez* Oil Spill Gulf Ecosystem  
Monitoring and Research Project Final Report

Biophysical Observations Aboard Alaska Marine Highway System Ferries

Gulf Ecosystem Monitoring and Research Project 040699  
Final Report

Edward D. Cokelet<sup>1</sup>  
Calvin W. Mordy<sup>2</sup>  
Antonio J. Jenkins<sup>2,3</sup>  
W. Scott Pegau<sup>4,5</sup>

<sup>1</sup>National Oceanic and Atmospheric Administration  
Pacific Marine Environmental Laboratory  
7600 Sand Point Way NE  
Seattle, WA 98115

<sup>2</sup>University of Washington  
Joint Institute for the Study of the Atmosphere and Ocean  
7600 Sand Point Way NE  
Seattle, WA 98115

<sup>3</sup>Current address:  
Coastal Environmental Systems, Inc.  
820 First Avenue South  
Seattle, WA 98134

<sup>4</sup>Alaska Department of Fish and Game  
Kachemak Bay Research Reserve  
95 Sterling Highway, Suite 2  
Homer, AK 99603

<sup>5</sup>Current address:  
Prince William Sound Science Center  
300 Breakwater Avenue  
P.O. Box 705  
Cordova AK 99574

29 July 2010

The *Exxon Valdez* Oil Spill Trustee Council administers all programs and activities free from discrimination based on race, color, national origin, age, sex, religion, marital status, pregnancy, parenthood, or disability. The Council administers all programs and activities in compliance with Title VI of the Civil Rights Act of 1964, Section 504 of the Rehabilitation Act of 1973, Title II of the Americans with Disabilities Act of 1990, the Age Discrimination Act of 1975, and Title IX of the Education Amendments of 1972. If you believe you have been discriminated against in any program, activity, or facility, or if you desire further information, please write to: EVOS Trustee Council, 441 West 5th Avenue, Suite 500, Anchorage, Alaska 99501-2340; or O.E.O. U.S. Department of the Interior, Washington, D.C. 20240.

*Exxon Valdez* Oil Spill Gulf Ecosystem  
Monitoring and Research Project Final Report

Biophysical Observations Aboard Alaska Marine Highway System Ferries

Gulf Ecosystem Monitoring and Research Project 040699  
Final Report

Edward D. Cokelet<sup>1</sup>  
Calvin W. Mordy<sup>2</sup>  
Antonio J. Jenkins<sup>2,3</sup>  
W. Scott Pegau<sup>4,5</sup>

<sup>1</sup>National Oceanic and Atmospheric Administration  
Pacific Marine Environmental Laboratory  
7600 Sand Point Way NE  
Seattle, WA 98115

<sup>2</sup>University of Washington  
Joint Institute for the Study of the Atmosphere and Ocean  
7600 Sand Point Way NE  
Seattle, WA 98115

<sup>3</sup>Current address:  
Coastal Environmental Systems, Inc.  
820 First Avenue South  
Seattle, WA 98134

<sup>4</sup>Alaska Department of Fish and Game  
Kachemak Bay Research Reserve  
95 Sterling Highway, Suite 2  
Homer, AK 99603

<sup>5</sup>Current address:  
Prince William Sound Science Center  
300 Breakwater Avenue  
P.O. Box 705  
Cordova AK 99574

29 July 2010

**Study History:** The Gulf of Alaska Ecosystem Monitoring and Research Program (GEM) funded this work as Project 040699 beginning in October 2003. The Alaska Marine Highway System (AMHS) generously allowed the project scientists to instrument the Alaskan ferry *Tustumena*, and a computer display terminal was installed aboard to explain the research and show the observations to passengers. The project was funded primarily by GEM through 31 December 2006, supplemented by support from PMEL and KBRR. The North Pacific Research Board (NPRB) picked up funding for one year, 1 August 2007-31 July 2008. Four Annual Reports (2004, 2005, 2006 & 2007) precede this Final Report. Several talks and posters pertaining to this work are listed in the Other References section below.

**Abstract:** An oceanographic measurement system aboard the Alaskan ferry *Tustumena* operated for four years in the Alaska Coastal Current with funding from the Exxon Valdez Oil Spill Trustee Council, the North Pacific Research Board and the National Oceanic and Atmospheric Administration. Sampling water from the ship's sea chest at 4 m, the underway system measured: (1) temperature and salinity – basic physical variables, (2) nitrate – an essential phytoplankton nutrient, (3) chlorophyll fluorescence – an indicator of phytoplankton concentration, (4) colored dissolved organic matter fluorescence – an indicator of terrestrial runoff, and (5) optical beam transmittance – an indicator of suspended sediment. The measurements show large spatial variability at short time scales, but spatially coherent climate change over annual time scales. Governed by snow and ice melt, the ocean climate transitioned from a warm, fresh regime in 2004-2005 to a cold, salty regime in 2007-2008. Agreement with observations at the GAK1 monitoring site near Seward, AK, extends their applicability to the northern Gulf of Alaska's continental shelf. Nitrate and chlorophyll measurements show nutrient-rich periods lead to increased phytoplankton. A computer monitor displayed the water temperature along the route and mapped the ferry's progress. The successful measurement program and connections to long-term climate change demonstrate the utility of oceanographic measurements from ferryboats.

**Key Words:** Alaska Coastal Current, CDOM, chlorophyll, ferry box, fluorescence, Gulf of Alaska, nitrate, oceanography, salinity, transmittance, *Tustumena*, volunteer observing ship, water temperature.

**Project Data:** This project measured oceanographic variables from an underway seawater system aboard the Alaska Marine Highway System ferry *Tustumena* sailing three primary routes: (1) year-around between Homer and Kodiak with short side trips to Seldovia and Port Lions, (2) biweekly trips during April to September between Kodiak and Dutch Harbor, and (3) from 15 September 2004 to 29 September 2005, three- to five-day trips between Kodiak, Seward and one or more Prince William Sound ports (Chenega Bay, Valdez and Cordova). The measurements continued until 6 November 2008 with funding from the North Pacific Research Board (NPRB). Water was pumped from the ship's sea chest at approximately 4 m depth and through a series of instruments to measure the following:

1. water temperature and salinity – basic physical parameters,
2. dissolved nitrate concentration – an essential nutrient for phytoplankton growth,
3. chlorophyll fluorescence – an indicator of chlorophyll concentration and phytoplankton biomass,
4. colored dissolved organic matter (CDOM) concentration - an indicator of dissolved substances, or yellow substances, released from tannins in decaying detritus, often of terrestrial origin, and
5. optical beam transmittance – an indicator of particulate concentration.

The measurements were made while underway every 30 seconds, except for the nitrate concentration which was measured every 10 minutes. Measurements ceased in port when the vessel was stationary.

The data are in two network Common Data Format (NetCDF) files, one for the nitrate measurements and the other for the remaining measurements. According to the NetCDF web site (<http://www.unidata.ucar.edu/software/netcdf>), “NetCDF (network Common Data Format) is a set of software libraries and machine-independent data formats that support the creation, access, and sharing of array-oriented scientific data.” The machine-independent nature of NetCDF files makes them particularly useful for data transfer and use on common computing platforms. Our data are array-oriented because the values are equally spaced with time (in GMT or UTC) as the independent variable. There are various conventions for NetCDF data. Our data sets were edited and created by the Ferret data visualization and analysis software (<http://ferret.wrc.noaa.gov/Ferret/>) and conform to the COARDS NetCDF convention (<http://www.unidata.ucar.edu/software/netcdf/conventions.html>). Presently some of the data are available in graphical form on this project’s web site ([http://www.pmel.noaa.gov/foci/GEM/alaska\\_ferry/GEM\\_ferry.html](http://www.pmel.noaa.gov/foci/GEM/alaska_ferry/GEM_ferry.html)). Researchers may request data copies from the Principal Investigator (Edward D. Cokelet, NOAA/PMEL, 7600 Sand Point Way NE, Seattle, WA 98115, (206) 526-6820, [Edward.D.Cokelet@noaa.gov](mailto:Edward.D.Cokelet@noaa.gov)). The data will be transmitted to US National Oceanographic Data Center (<http://www.nodc.noaa.gov/>) in FY2010. Under a grant from NPRB, the data will be made available in FY2010 on the project’s web site.

**Citation:**

Cokelet, E. D., C. W. Mordy, A. J. Jenkins and W. S. Pegau, 2010. Biophysical Observations Aboard Alaska Marine Highway System Ferries, *Exxon Valdez* Oil Spill Gulf Ecosystem Monitoring and Research Project Final Report (Gulf Ecosystem Monitoring and Research Project 040699), Alaska Department of Fish and Game, Habitat Restoration Division, Anchorage, Alaska.

## **Table of Contents:**

	Page
Title Page	3
Study History	4
Abstract	4
Key Words	4
Project Data	4
Citation	5
Table of Contents	6
List of Tables	6
List of Figures	6
List of Appendices	8
Executive Summary	9
Introduction	11
Objectives	13
Methods	16
Results	31
Discussion	47
Conclusions	59
Outreach	59
Acknowledgements	60
Appendix	61
Literature Cited	64
Other References	66

## **List of Tables:**

Table 1. Oceanographic Instrumentation on *Tustumena*.

## **List of Figures:**

Figure 1. The Alaska Marine Highway System ferry *Tustumena*. Photo by Mary Glover, Seldovia, AK.

Figure 2. The *Tustumena*'s route between Homer and Kodiak with less frequent trips to Prince William Sound and Dutch Harbor.

Figure 3. The chlorophyll front surrounding Kodiak Island from SeaWIFS images composited from June through August of 1998 to 2002.

Figure 4. Schematic diagram of the underway seawater sampling system.

Figure 5. The main instrument box of the underway seawater sampling system.

- Figure 6. Thermosalinograph salinity calibration from water bottle samples.
- Figure 7. ISUS nitrate calibration from discrete water bottle samples before the shutter-dust fouling problem was discovered.
- Figure 8. ISUS nitrate calibration from discrete water bottle samples after the shutter-dust fouling problem was rectified.
- Figure 9. Fluorometer chlorophyll calibrations from discrete water samples for (a) the WETStar in 2005, and the ECO fluorometers in (b) 2006, (c) 2007 and (d) 2008.
- Figure 10. Time series of the optical beam transmittance,  $T_r$ , of ocean water (black curve), fresh water during backflushes (red curve) and the maximum fresh-water backflush values,  $T_{r_{fw}}$  (green curve) during September 2006. Also shown is the ratio of the ocean to fresh water transmittance (blue curve).
- Figure 11. Time series of *Tustumena*'s sea chest intake temperature at 4 m depth.
- Figure 12. Map of the water temperature along *Tustumena*'s route on 12-14 July 2005.
- Figure 13. Time series of *Tustumena*'s salinity at 4 m depth.
- Figure 14. Map of the salinity along *Tustumena*'s route on 12-14 July 2005.
- Figure 15. The near-surface temperature measured at GAK1 from CTD measurements and *Tustumena*'s underway system.
- Figure 16. The near-surface salinity measured at GAK1 from CTD measurements and *Tustumena*'s underway system.
- Figure 17. Temperature and salinity measured in Resurrection Bay from *Tustumena* on 16-17 June 2005 showing the location of the GAK1 CTD site relative to the ship track.
- Figure 18. Time series of *Tustumena*'s dissolved nitrate concentration at 4 m depth.
- Figure 19. The nitrate concentration along *Tustumena*'s ship track in the Gulf of Alaska during one of its infrequent late-deployment trips into Prince William Sound on 15-17 April 2008.
- Figure 20. Time series of *Tustumena*'s chlorophyll concentration at 4 m depth

- Figure 21. The inferred phytoplankton carbon concentration plotted against the nitrogen (from nitrate) concentration for the March-May 2005-2008 *Tustumena* measurements.
- Figure 22. Time series of *Tustumena*'s CDOM concentration at 4 m depth.
- Figure 23. The CDOM concentration along *Tustumena*'s track on 7 July 2008 shows the highest values near Kodiak.
- Figure 24. Time series of *Tustumena*'s attenuation coefficient difference,  $c - c_{fw}$ , between seawater at 4 m depth and fresh water.
- Figure 25. Map of the attenuation coefficient difference along *Tustumena*'s route on 12-14 July 2005.
- Figure 26. The temperature climatology for on Kachemak Bay, Kennedy Entrance, the Barren Islands and Marmot Strait.
- Figure 27. The temperature anomaly for Kachemak Bay, Kennedy Entrance, the Barren Islands, Marmot Strait, the Kodiak-Homer route and GAK1.
- Figure 28. The salinity climatology centered on Kachemak Bay, Kennedy Entrance, the Barren Islands and Marmot Strait.
- Figure 29. The salinity anomaly for Kachemak Bay, Kennedy Entrance, the Barren Islands, Marmot Strait, the Kodiak-Homer route and GAK1.
- Figure 30. The Pacific Decadal Oscillation (PDO) index during the *Tustumena* measurement period.
- Figure 31. The nitrate climatology for Kachemak Bay, Kennedy Entrance, the Barren Islands and Marmot Strait.
- Figure 32. The nitrate anomaly for Kachemak Bay, Kennedy Entrance, the Barren Islands, Marmot Strait and the Kodiak-Homer route.
- Figure 33. The chlorophyll climatology for Kachemak Bay, Kennedy Entrance, the Barren Islands and Marmot Strait.
- Figure 34. The chlorophyll anomaly for Kachemak Bay, Kennedy Entrance, the Barren Islands, Marmot Strait and the Kodiak-Homer route.

**List of Appendices:**

Appendix - Details of the Underway Seawater Monitoring System Control

**Executive Summary:** The *Exxon Valdez* Oil Spill Trustee Council's Gulf of Alaska Ecosystem Monitoring and Research Program (GEM), the North Pacific Research Board (NPRB) and the National Oceanic and Atmospheric Administration's Pacific Marine Environmental Laboratory (NOAA/PMEL) funded an oceanographic measurement system aboard the Alaska Marine Highway System (AMHS) ferry *Tustumena*. The project's goal was to use this Volunteer Observing Ship to establish a long-term monitoring program to detect environmental change and to expand the understanding of Gulf of Alaska ecosystems. The objectives were to consult with AMHS, design and install an automated, oceanographic sampling system on *Tustumena*, and initiate a long-term monitoring program of physical and biological time series in the Alaska Coastal Current (ACC). These objectives were achieved. The oceanographic measurement system aboard *Tustumena* operated for four years in the Alaska Coastal Current.

Sampling water at 4 m, the underway system measured: (1) temperature and salinity – basic physical variables, (2) nitrate – an essential phytoplankton nutrient, (3) chlorophyll fluorescence – an indicator of phytoplankton concentration, (4) colored dissolved organic matter (CDOM) fluorescence – an indicator of terrestrial runoff, and (5) optical beam transmittance – an indicator of suspended sediment. The system was designed to operate remotely for days at a time. Data were collected every 30 seconds (or 10 minutes for nitrate) and sent back hourly to PMEL via Iridium satellite modem. Several times each year, scientists rode the ship to collect discrete water samples for laboratory analyses of salinity, nitrate and chlorophyll. These were applied with care to calibrate the underway electronic instruments.

A computer display in the ship's passenger lounge provided a platform for public outreach. It gave a changing slide show consisting of background material, the real-time temperature along the ship's cruise track, the ship's location on a map, and periodic Google Earth virtual fly-overs of the geographic features around the ship's location. Also nine talks or posters were presented at scientific conferences over the project's duration.

The results were time series measurements of the water temperature, salinity, nitrate, chlorophyll, CDOM, and optical beam transmittance across the Alaska Coastal Current with most of the observations being made between Homer and Kodiak. The measurements varied more rapidly with distance along the ferry route than with time at a fixed locale as the ship steamed from sheltered harbors with melt water runoff to the open ocean. In an overall sense, the annual cycle varied from relatively cold, salty conditions in winter to warm, fresh conditions in summer due to solar warming and melt water runoff. Nitrate was high in winter – having been mixed up from deep layers by storms – and decreased in spring and summer owing to phytoplankton utilization. Chlorophyll was low in winter, rose in spring with the increased sunlight and available nutrients, and then decreased in summer as nutrients were consumed by phytoplankton. CDOM was high in spring and fell off with autumn. Optical transmittance changes owing to sedimentary particles showed relatively little seasonal variation and were governed by local conditions with higher values in harbors due to local runoff and lower values offshore.

The measurements show large spatial variability at short time scales, but spatially coherent climatic anomalies persist over annual and longer time scales. Governed by snow and ice melt, the ocean climate transitioned from a warm, fresh regime in 2004-2005 to a cold, salty regime in 2007-2008. Agreement with temperature and salinity observations at the GAK1 long-term monitoring site near Seward, AK, extends the applicability of those measurements to the northern Gulf of Alaska's continental shelf. *Tustumena* nitrate and chlorophyll measurements show nutrient-rich periods lead to increased phytoplankton. The successful measurement program and connections to long-term climate change demonstrate the utility of oceanographic measurements from ferryboats.

**Introduction:** In 1999 the *Exxon Valdez* Oil Spill Trustee Council began preparations for the Gulf of Alaska Ecosystem Monitoring and Research Program. One goal was to establish a long-term monitoring program to detect environmental change and to expand the understanding of Gulf of Alaska ecosystems. GEM monitoring would complement that of other resource agencies and research institutions. Monitoring at sea is expensive if done from a dedicated research vessel that can cost upwards of \$20,000 per day to operate; however other alternatives exist. One is to use a vessel that plies the waters of interest and outfit it to make scientific measurements. Such a Volunteer Observing Ship operates at no cost to the research agency. The Alaska Marine Highway System operates a fleet of ferries in Alaska. The ferry *Tustumena* (Figure 1) crosses the Alaska Coastal Current between the Kenai Peninsula and Kodiak Island over 280 times per year with less-frequent trips northeast into Prince William Sound and southwest to Dutch Harbor (Figure 2). Recognizing this, GEM made it a top priority for FY2004 to begin the process of collecting basic physical and biological observations from an Alaskan ferry. They sought proposals for a design feasibility study. The National Oceanic and Atmospheric Administration's Pacific Marine Environmental Laboratory and the Alaska Department of Fish and Game's Kachemak Bay Research Reserve (ADF&G KBRR) responded jointly with an actual design and proposed to build and operate an oceanographic monitoring system on *Tustumena*.



Figure 1. The Alaska Marine Highway System ferry *Tustumena*. Photo by Mary Glover, Seldovia, AK.

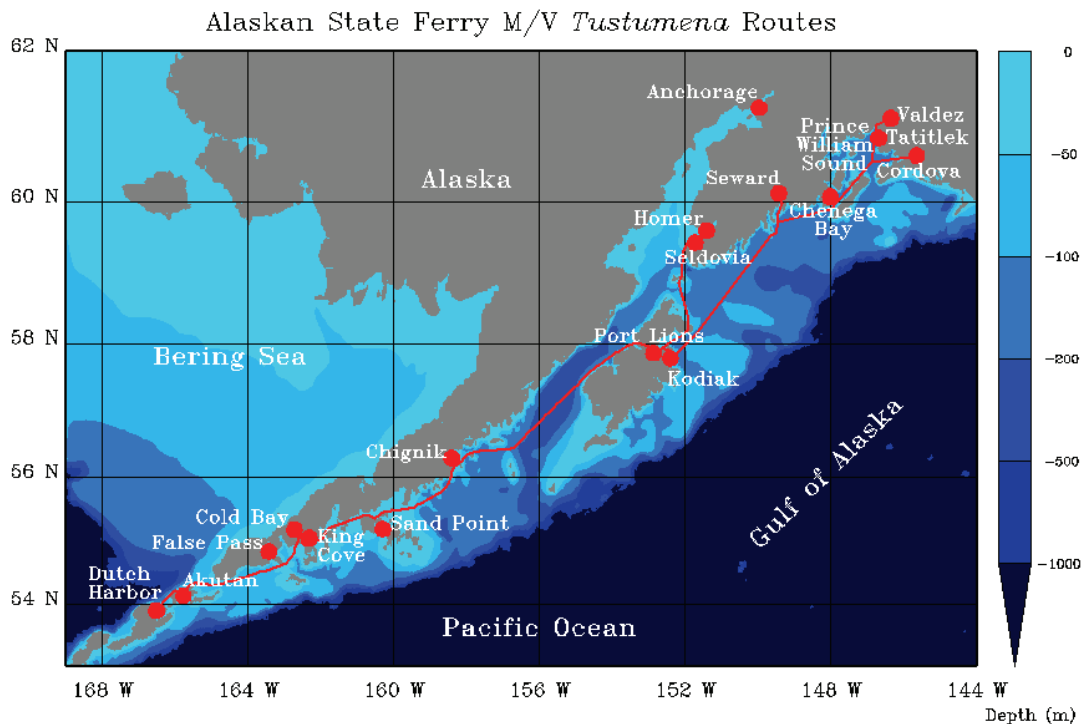


Figure 2. The *Tustumena*'s route between Homer and Kodiak with less frequent trips to Prince William Sound and Dutch Harbor.

GEM funded the PMEL-KBRR proposal, and work began in October 2003 with system design and instrument procurement. We used off-the-shelf oceanographic instruments and designed plumbing, data acquisition and telemetry systems to meet our needs. After testing during spring and summer 2004, measurements began on 15 September 2004 and continued under GEM funding until 31 December 2006, under PMEL and KBRR funding until August 2007 and then under NPRB funding to 6 November 2008.

This project's principal results are as follows:

1. We successfully designed, built, installed and operated an underway-oceanographic observing system on the Alaskan ferry *Tustumena*.
2. The system had the following novel features:
  - a. Hourly data transmittal to PMEL via Iridium satellite,
  - b. Two-way Iridium satellite communication between the data acquisition system and PMEL,
  - c. Leak detection with automatic seawater supply cut off,
  - d. Freshwater backflushing upon arrival in ports to increase the time between manual cleanings,

- e. Automatic cessation of measurements while in ports to conserve data transmission and storage,
  - f. Automatic e-mail notification of system problems,
  - g. A passenger display terminal showing the ferry position and the latest oceanographic measurements, and
  - h. Successful application of an optical sensor to measure dissolved nitrate concentrations on an underway system.
3. We measured a four-year time series of near-surface oceanographic properties over a 1000 km of ferry route in the Gulf of Alaska.
  4. The longevity of the measurements was sufficient that multiyear monthly means and their anomalies have been calculated, and climatic signals emerge.
  5. Similarity to the temperature and salinity anomalies at GAK1 prove that long-term climate measurements there apply to a wide region of the Gulf of Alaska.
  6. Temperature and salinity anomalies in the Alaska Coastal Current transitioned from relatively warm, fresh ocean conditions to cool, salty ones during the *Tustumena* measurement period.
  7. New nitrate and chlorophyll anomalies indicate that relatively higher nutrients coincide with a greater phytoplankton stock and vice versa.

**Objectives:** The goal of the proposed research was to install an automated underway-oceanographic sampling system on the Alaska ferry *Tustumena* to obtain high-resolution surface maps of physical and biochemical properties across the Alaska Coastal Current (ACC) and across the chlorophyll front (Figure 3) on the seaward side of Kodiak Island. The front would be intersected obliquely during the ferry's regular transits between Kodiak Island and Seward or Prince William Sound ports. The specific objectives of this research were as follows:

**Objective 1:** Consult with AMHS, design and install an automated, oceanographic sampling system on the *Tustumena*.

**Hypothesis:** It is possible to design an automated, seawater-sampling system that meets both scientific goals and ship's safety concerns.

Objective 1 was fully met. The oceanographic system was designed following consultations with AMHS and a naval architect. Installation began in Spring 2004. It became operational on 15 September 2004 and continued to operate to 6 November 2008 except during periods of shipyard repair and instrument failure or refurbishment. This is our main operational result.

**Objective 2:** Initiate a long-term monitoring program of physical and biochemical time series in the ACC.

**Hypothesis:** Such time series will establish the annual variability in the ACC and lead toward measuring interannual and decadal trends in the ecosystem. The measurements will also provide high-resolution, temporal data to resource-modeling teams.

Objective 2 was fully met. With four years of measurements, we can begin to establish their mean annual cycles and anomalies. We have shown that the anomalies have a regional scale and can be detected from near-surface oceanographic measurements on an Alaskan ferry. Departures from the October 2004-October 2008 mean show cold, fresh years and warm, salty years that are felt across the ACC between Homer and Kodiak. This is our main scientific result. Future years of measurements would better define the annual cycle, its variation and climatological trends. The observations would allow us to create climatic ecosystem indices based upon a variety of actual oceanographic measurements made directly in the ACC. These would complement other climate indices, but might be more relevant because they would not be confined, for example, to atmospheric measurements or to the limited set of parameters observed by satellites under clear skies.

**Objective 3:** Map the surface temperature, salinity, nitrate, optical transmittance, chlorophyll fluorescence and colored dissolved organic matter on *Tustumena* transits across the chlorophyll front seaward of Kodiak Island on the Kodiak-Seward and Kodiak-Prince William Sound routes and characterize the seasonal development of the front as shown in Figure 3.

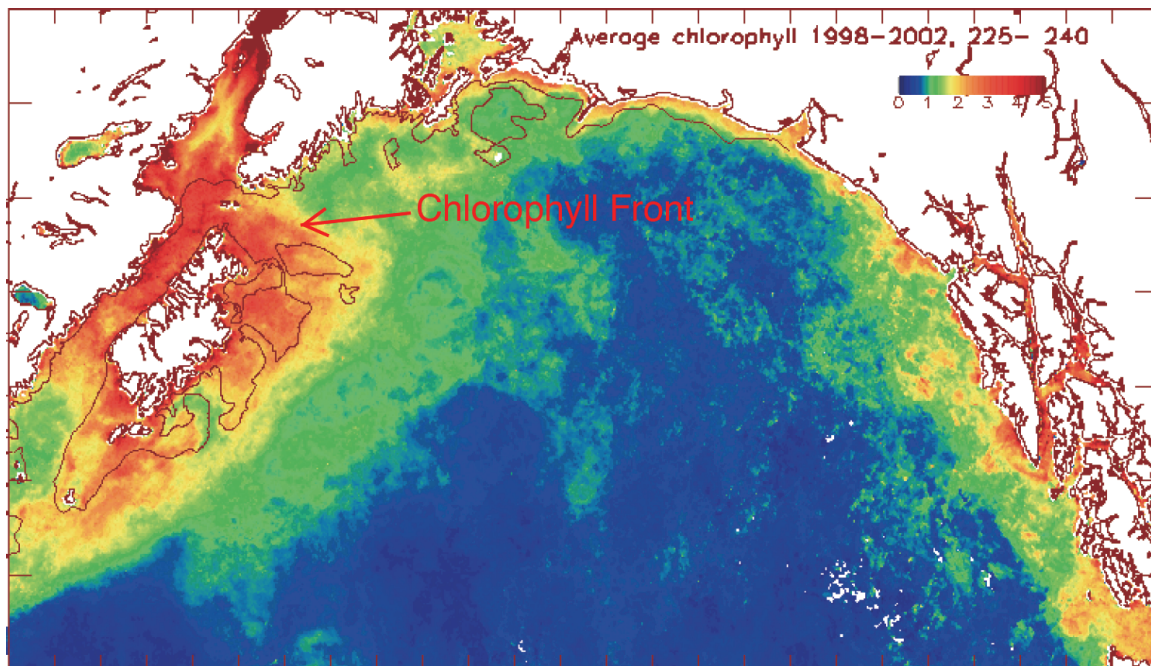


Figure 3. The chlorophyll front surrounding Kodiak Island from SeaWiFS images composited from June through August of 1998 to 2002.

Hypothesis: In summer, surface waters southeast of the Kenai Peninsula are depleted in nitrate and chlorophyll; whereas mixing over shoals off Kodiak Island and in lower Cook Inlet sustains post-bloom production. The result is the seasonal development of a chlorophyll front.

Objective 3 was not fully met because beginning 1 October 2005, the Alaska Marine Highway System altered *Tustumena*'s route, removing Seward and Prince William Sound destinations. *Tustumena* remained on the Homer-Kodiak route and did not sail across the chlorophyll front regularly until less-frequent service resumed between Kodiak and Prince William Sound ports on 19 November 2007 after GEM funding had ended. We were not able to pursue this objective fully because we could only collect data from the first year of the study.

## **Methods:**

We designed, built, installed and operated the underway seawater sampling system on *Tustumena* – a 296 ft (90 m) car and passenger ferry displacing 3,067 long tons (Figure 1). Work began before the project was funded when two of us (E. D. Cokelet and A. J. Jenkins) toured *Tustumena* in Kodiak on 16 July 2003 to investigate possible sites where seawater could be drawn from a sea chest for sampling. The captain and crew were very helpful, and Chief Engineer Ken Hammer suggested the best site as being in the port shaft alley. There, a sea chest supplied seawater for sanitation and fire fighting, space was adequate for instrument mounting, and a freshwater supply was available for back flushing the instruments. Safety was a concern because we proposed to tap into a seawater line leading from the ship's hull, and a catastrophic leak could sink the ship. Antonio Jenkins produced a preliminary design that was reviewed by a naval architecture firm – Art Anderson Associates, Seattle – and modified to produce a final design that met American Bureau of Shipping standards, as required by AMHS.

**System Design:** The underway seawater observing system consisted of several parts. Located in the ship's port shaft alley, a seawater intake line tapped off an existing sea-chest air vent whose inlet was approximately 4 m below the water line. Water flowed at about 3.3 L/min through 1.45 m of insulated 1-inch-diameter copper-nickel pipe, a manual shut-off valve, 0.31 m of bare pipe to an in-line digital temperature sensor, 0.31 m to a coarse sea strainer that removed marine debris, 0.51 m to a 1-to-1/2-inch reducer fitting and 3.40 m of 1/2-inch-diameter copper-nickel pipe to the self-contained main instrument box. The stainless steel instrument box was plumbed with a total of 6.40 m of 3/8-inch-diameter Tygon tubing. Within the box, seawater flowed through a flow meter, motorized shut-off valve, self-cleaning screen, 1/4-hp Hydra-Cell positive-displacement pump, stilling-well debubbler and to the instrument loop consisting of a flow meter, chlorophyll and colored dissolved organic matter (CDOM) fluorometers, optical transmissometer, 50  $\mu\text{m}$  and 1  $\mu\text{m}$  filters, optical nitrate sensor and thermosalinograph (Figures 4 and 5). Finally water was dumped into the bilge where the ship's pumps removed it. Table 1 lists the oceanographic instruments installed. A Linux computer was located in a waterproof section at the top of the main instrument box. It controlled the sampling via a LabVIEW program. Mounted above deck near the ship's bridge, a global positioning system (GPS) receiver computed the ship's position and an Iridium satellite modem sent data to PMEL. A second instrument box contained a marine-grade uninterruptible power supply and a Windows computer to drive a public graphical data display in the passenger lounge. The public display showed an image sequence describing the project and continuously updated maps of temperature along the ship's track. In a later version we added Google Earth images that showed the ship's position and periodically zoomed out and panned to show the surrounding terrain. Passengers and crew found this useful to monitor trip progress.

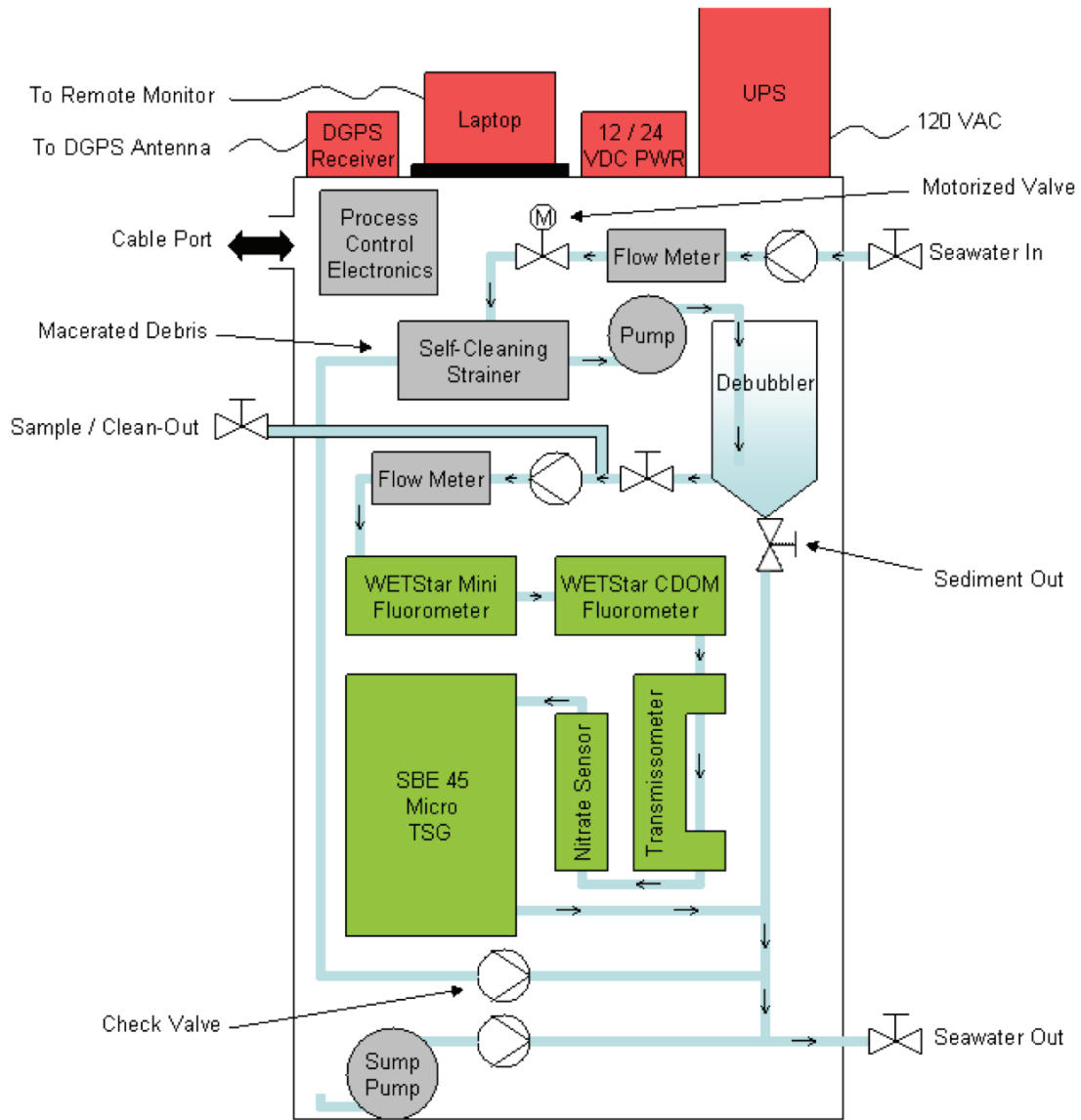


Figure 4. Schematic diagram of the underway seawater sampling system.

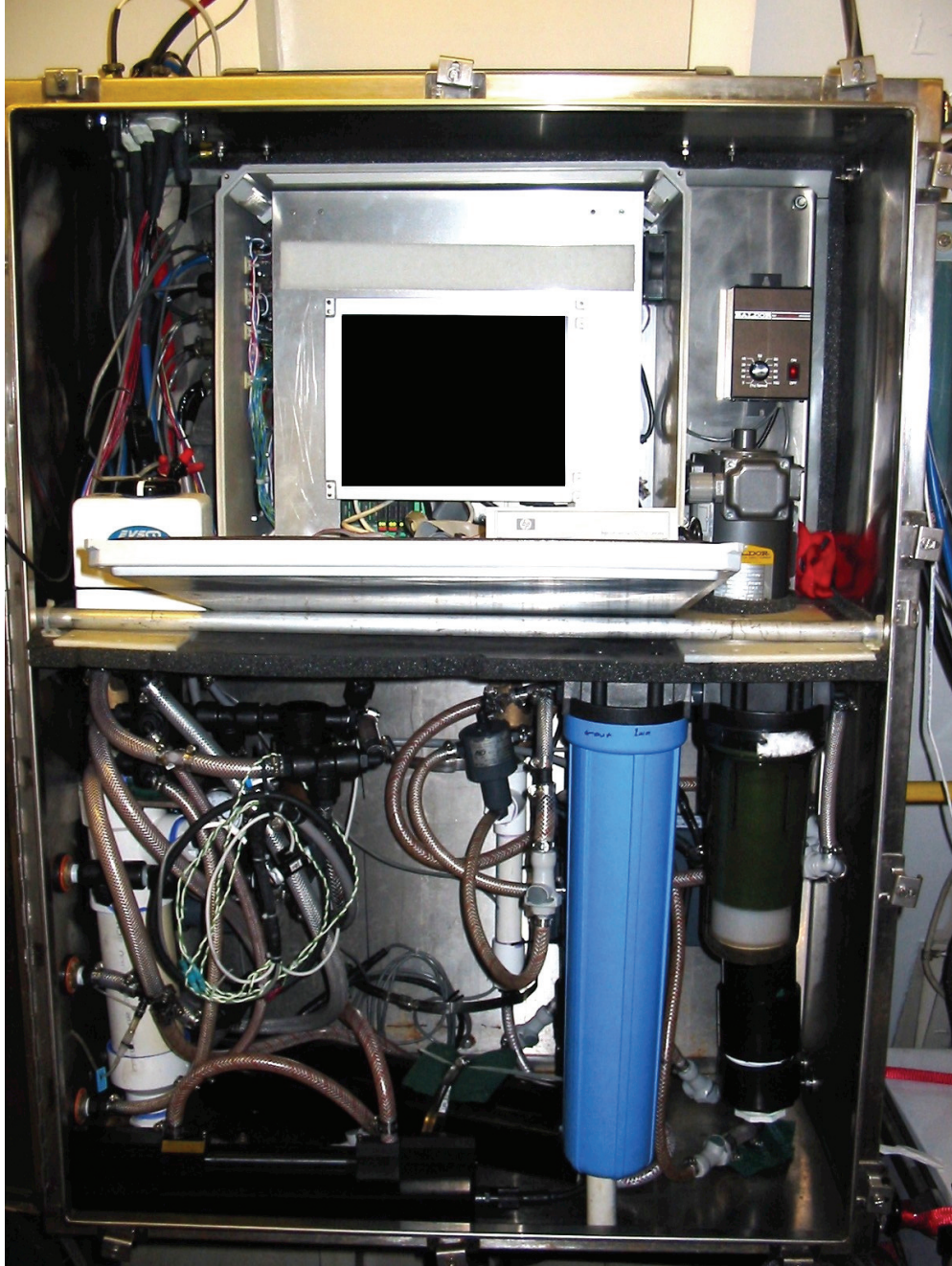


Figure 5. The main instrument box of the underway seawater sampling system.

Table 1. Oceanographic Instrumentation on *Tustumena*.

Parameter Measured	Instrument	Operating Period
Water temperature	Sea-Bird SBE 38 Digital Oceanographic Thermometer	15 Sep 2004 – 6 Nov 2008
Salinity	Sea-Bird SBE 45 MicroTSG Thermosalinograph	15 Sep 2004 – 6 Nov 2008
Dissolved nitrate concentration	Satlantic ISUS Nitrate Sensor	15 Sep 2004 – 6 Nov 2008
	EnviroTech Nutrient Analyzing System	30 Aug 2005 – 21 Nov 2005
Chlorophyll concentration	WET Labs WETStar (Chl) Fluorometer	15 Sep 2004 – 21 Nov 2005
	WET Labs ECO Chlorophyll Fluorometer	10 May 2006 – 6 Nov 2008
Colored Dissolved Organic Matter concentration	WET Labs WETStar (CDOM) Fluorometer	15 Sep 2004 – 14 Aug 2005
	WET Labs ECO CDOM Fluorometer	30 Jul 2006 – 6 Nov 2008
Particulate concentration	WET Labs C-STAR Transmissometer (25 cm)	15 Sep 2004 – 6 Nov 2008

The system was designed to operate remotely for days at a time. Data were collected and sent back hourly to PMEL via Iridium satellite modem. Also new instructions could be sent to the system via Iridium to change its sampling criteria and rates. When the ship arrived in port, the system sensed the lack of motion and entered Sleep Mode. The pump stopped to reduce the chance of sucking in marine debris, and measurements and data logging were suspended. In Sleep Mode the ship's position was monitored. When the ship began moving, the system entered Normal Mode and resumed measuring and logging. The Appendix gives the details of the control system.

Plumbing and electrical work began during the ship's annual shipyard period in March-April 2004 at Seward Ships Drydock. Owing to shipyard delays, this work was not completed until a 36-hour layover in Seward on 21 May 2004. Troubleshooting on the full system began in Summer 2004, and it became operational on 15 September 2004.

Problems: Three main types of problems were encountered: bubbles, Iridium modem lockup and fouling. During testing we found that when the ship reversed while docking, large volumes of air were entrained downward and forward into the sea chest. The debubbler was overwhelmed, and the pump air-locked. We solved this by adding two float-valve-actuated air vents (Spirovent air eliminators) commonly used on hot-water-

heating systems. At times the Iridium modem would lockup for no apparent reason. We wrote software to detect this condition and cycle power to the modem.

Fouling came from two sources – marine growth and rust. It was held at bay using several strategies: screens and filters, freshwater backflushing, instrument anti-fouling techniques and periodic manual cleaning. Seawater was screened via a coarse in-line strainer as used on marine engines and a backflushed fine screen. However small rust particles from the ship's hull could pass through these screens and coat the optical window of the ISUS nitrate sensor with a film that was opaque to ultraviolet light. Two domestic water filters (50  $\mu\text{m}$  and 1  $\mu\text{m}$ ) were installed to remove the rust particles in stages. The system automatically backflushed all tubing and instruments within the instrument box with fresh water before shutting down in port or whenever it sensed flow reductions due to fouling. See Appendix for details. Some of the instruments had anti-fouling capabilities built into them. The WET Labs ECO chlorophyll and CDOM fluorometers used bio-wipers to wipe their optical windows before sampling. The Sea-Bird thermosalinograph was equipped with a tributyltin antifoulant tablet. It was the last instrument in the flow line so that its antifoulant would not affect plankton fluorescence. Approximately weekly, personnel from KBRR boarded the ship in Homer, AK, to clean the sensors. At times, especially during rapid plankton growth, even these measures were inadequate to deal with fouling, and bad data had to be identified and removed.

Data Editing: GPS position, intake temperature, thermosalinograph temperature and salinity, chlorophyll and CDOM fluorescence, optical beam transmittance, pressure drop, and flow rate were recorded every 30 seconds and transmitted to PMEL without editing. Because the system could start up at any time, these data did not always fall at integer-multiples of 30 seconds on the clock. Hence they were linearly interpolated onto a regular, equispaced time axis at 30-second intervals. The instrumental measurements contained glitches owing to start-up transients, slow flow, failed sensors, dirty sensors, passing debris, power surges, transmission errors, etc. Usually bad values took the form of spikes, very low values or very high values. Therefore the data required some editing. Random position jumps were removed if they exceeded a  $1^\circ/\text{time step}$ . Time gaps longer than 4 time steps were identified and the first 14 time steps after each gap were ignored to eliminate start-up transients. By trial and error, a general criterion to remove bad values from all the 30-second data was developed based upon a combination of flow-rate, temperature difference, and salinity values and spikes. Values were eliminated if (a) the flow rate was less than a flow-meter-dependent threshold, (b) the difference between the intake and thermosalinograph temperatures exceeded  $3^\circ\text{C}$ , (c) the salinity was less than 2 psu, or (d) salinity jumps exceeded  $0.5 \text{ psu}/\text{time step}$ . In addition, bad chlorophyll fluorescence values were eliminated if the fluorescence voltage was negative or changed by less than 0.0001 or more than  $1.2 \text{ V}/\text{time step}$ . The CDOM measurements in 2004 through July 2006 made with WETStar fluorometers were neglected because they were negative and very much lower than in 2007-2008. The remaining 2006 measurements were dropped because they were noisy and had spurious jumps and trends. CDOM spikes were eliminated if the values changed by more than  $6 \text{ ppb}/\text{time step}$ . Optical transmittance spikes were eliminated if the values changed by more than  $2 \text{ V}/\text{time step}$ . The automated data editing techniques worked well. However for final quality control,

graphs of all data were scrutinized visually, and some additional values were eliminated by subjective evaluation. After automatic and subjective editing, 9% of the temperature, salinity and optical transmittance data and 31% of the fluorescence data were edited out of the final data set. Most of the bad fluorescence data came from the first year before self-cleaning fluorometers were installed.

ISUS nitrate concentration and associated data-quality parameters were sampled every 10 minutes to allow the ultraviolet bulb to last the length of the project. This instrument was newly developed and, to our knowledge, had not been used successfully in an underway system before. We developed three error thresholds based upon (a) the instrument's own nitrate error estimate, (b) the difference between its salinity estimate and the thermosalinograph salinity, and (c) the spectral average over the measurement wavelength band. These thresholds changed between deployments as the manufacturer improved the instrument. Observations degraded as the strength of the optical signal decreased due to fouling of the optics. The measurements bounced back after cleaning. Our data editing eliminated 23% of the data, but most of this was in the first year before the manufacturer found that particles shed from the instrument's shutter fouled the optics internally.

Calibration: Instruments must be calibrated to ensure measurement accuracy. Typically *Tustumena* entered the shipyard for routine maintenance for over a month between late fall and early spring each year. We usually removed the instruments at that time and returned them to their manufacturers for checking, calibration and refurbishment. Several times each year, project personnel rode the ferry from Homer to Kodiak and back to extract discrete water samples from the sampling port for calibration purposes.

Ocean temperature was measured near the seawater intake with a remote digital thermometer (Table 1). The manufacturer's temperature bath calibrations showed the remote temperature sensor's absolute mean residual error was 0.00035°C, and it drifted less than 0.00052°C/yr. This instrumental error is negligible compared to other sources of bias and the natural variability of the measurements. We estimate that the water warmed negligibly as it passed under *Tustumena*'s 90-m-long hull at an average speed of 6.8 m/s (13 kt) requiring 13 seconds to reach the sea chest. It is difficult to estimate how much the water temperature changed as the water flowed from the seawater intake in its 1-inch-diameter ( $D = 2r = 2.54$  cm) pipe for a length  $L (=176$  cm) to the remote temperature sensor, but we can put an upper bound on that value. The average flow speed in the pipe ( $u$ ) is given by the ratio of the volume flow rate ( $[3.3$  L/min][1000 cm<sup>3</sup>/l][min/60 s] = 55 cm<sup>3</sup>/s) to the cross-sectional area ( $\pi r^2 = \pi [1.27$  cm]<sup>2</sup> = 5.07 cm<sup>2</sup>) and equals 10.9 cm/s. The transit time from the sea chest to the temperature sensor was 16.2 s. The heat transfer from the water to the pipe to the surrounding air depends upon the Reynolds and Nusselt numbers of the flow, the pipe material and thickness, and the pipe's outer wall temperature (Lienhard, J. H., IV and Lienhard, J. H., V, 2008). The pipe-flow Reynolds number  $R (= uD/\nu$  where  $\nu$  is the kinematic viscosity of water  $\approx 0.0124$  cm<sup>2</sup>/s), was 2200, which means that the flow was transitioning from laminar to turbulent. We used Lienhard and Lienhard (2008, Chapter 7) to compute the Nusselt

number and the fluid heat transfer coefficient,  $h_F = 240 \text{ W/m}^2\text{K}$ , at the deployment-averaged temperature of  $7^\circ\text{C}$ . The net heat transfer coefficient,  $h$ , of the system is given by the inverse of the mean inverse heat transfer coefficients for each step of the transfer process, i.e.  $1/h = 1/h_F + 1/h_p + 1/h_i$  where  $h_w$ ,  $h_p$  and  $h_i$  are the heat transfer coefficients for the water, pipe and insulation surrounding it. The heat transfer coefficient for the Cu-Ni pipe (Powell, C. A., 2010) is the ratio of its thermal conductivity ( $29 \text{ W/mK}$ ) to its wall thickness ( $5/32 \text{ inches} = 3.97 \times 10^{-3} \text{ m}$ ) which gives  $h_p = 7300 \text{ W/m}^2\text{K}$ . The pipe was insulated by  $3/8$ -inch-thick foam insulation with an R-value of 2 which by the definition of a US R unit ( $R = 0.176 \text{ Km}^2/\text{W}$ ) gives  $h_i = 2.84 \text{ W/m}^2\text{K}$ . The pipe insulation was not always fully in place, so the overall heat transfer coefficient,  $h$ , varied between 232 and  $2.84 \text{ W/m}^2\text{K}$  depending upon the absence or presence of the insulation. The temperature  $T$  a distance  $L$  from the sea with intake temperature  $T_0$  is given by (Lienhard, J. H., IV and Lienhard, J. H., V, 2008, eqn 7.59b)

$$\frac{T - T_0}{T_w - T_0} = 1 - \exp\left(-\frac{4hL}{\rho u C_p D}\right) \quad (1)$$

where  $T_w$  is the temperature at the outer wall of the pipe or insulation,  $\rho$  is the water density, and  $C_p = 4200 \text{ J/kgK}$  is the heat capacity of the fluid. Substituting values into equation (1) and rearranging gives  $T - T_0 = 0.13(T_w - T_0)$  for bare pipe and  $T - T_0 = 0.0017(T_w - T_0)$  for insulated pipe. Unfortunately the outer wall temperature,  $T_w$ , was not measured; therefore we must estimate it. The ship's shaft alley temperature tended toward the sea temperature because it was below the water line and surrounded by water on three sides. The compartment was heated at times, but the seawater pipe was located below the floorboards near the ship's hull. The bare pipe always felt cold to the touch owing to the cold water flowing in it. For the case of a bare pipe, we estimate that  $T_w$  did not exceed  $T_0$  by more than  $2^\circ\text{C}$ . In that case an upper limit on the temperature increase would be  $0.26^\circ\text{C}$ . With the pipe insulation in tact, an extreme upper limit for the insulation's outer wall temperature would be the room temperature, say  $20^\circ\text{C}$ , and a lower limit for the inlet temperature would be  $0^\circ\text{C}$ . Therefore, an upper bound on the temperature increase between the sea and the temperature sensor,  $T - T_0$ , would be  $0.034^\circ\text{C}$  for insulated pipe. We do not know when the pipe insulation was in place or removed. As the temperature measurements will show in the Results section, a bias of  $0.26^\circ\text{C}$  is small compared to temperature variability along the ship's track and between years. A bias of  $0.034^\circ\text{C}$  for insulated pipe is negligible.

Ocean salinity was measured via thermosalinograph in the main instrument box (Table 1). The thermosalinograph actually measures conductivity, which is corrected by the temperature at the measurement point to give salinity. When new or after refurbishment, the salinity sensors had negligible error at the factory. Post-deployment factory tests revealed drifts of  $-0.024$  to  $-0.115 \text{ psu/year}$  that were smaller than the natural variability encountered. These tests were used to show that the sensors were working correctly. For salinity calibration, water samples were collected from the underway system's sampling port, stored in triple-rinsed 200-ml Kimax borosilicate bottles and analyzed in the laboratory with a Guildline Autosal laboratory salinometer. Thermosalinograph salinities

measured at the time of water sampling were regressed against the bottle values as shown by the green line in Figure 6. The linear regression accounted for 96% of the variance. Based upon the student's t score statistic, the slope of the fit was significantly different from zero with over 99% confidence. The black symbols represent the acceptable data points, and the red symbols are outliers that were excluded from the fit. The final calibrated salinity was computed from the field calibrations via the inverse fit equation, e.g.  $S = 1.008 S_{TSG} - 0.0614$ . The standard error of the  $S_{TSG}$  estimate was 0.130 psu. The thermosalinograph salinity was typically lower than the bottle salinity by about 0.185 psu as shown by the displacement of the green line from the blue dashed line along which the data points would lie if the samples from the two sources matched exactly. We cannot explain why there is a displacement, but by employing field observations we can correct for it.

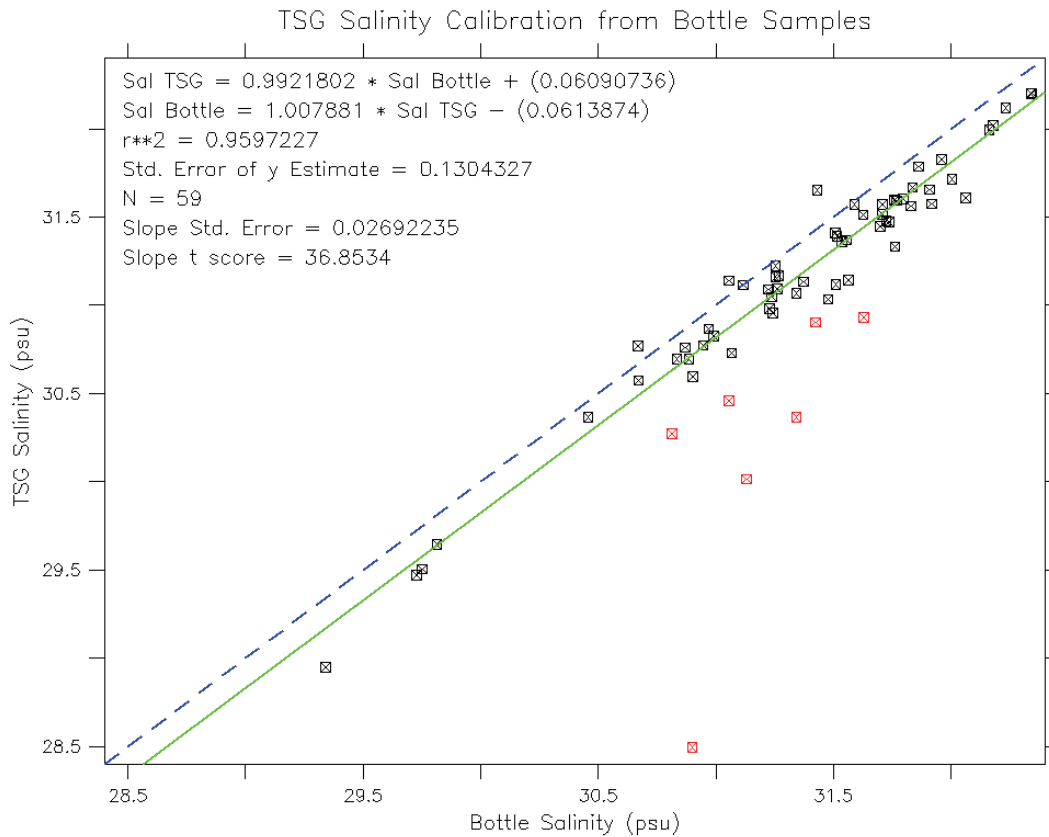


Figure 6. Thermosalinograph salinity calibration from discrete water bottle samples. Black symbols represent the data points, and red symbols are outliers excluded from the fit. The green line is the linear least squares fit, and the dashed blue line represents the line along which the data points would lie if the samples from the two sources matched exactly.

The concentration of dissolved nitrate, a phytoplankton nutrient, was measured with a Satlantic ISUS (in situ ultraviolet spectrophotometer) nitrate sensor employing optical ultraviolet absorption spectroscopy (Table 1). This was the first commercially available oceanic nitrate sensor that did not use chemicals and their attendant monitoring and renewal to measure nitrate, and ours was one of the first applications of this technology to an underway sampling system. The instrument was set up to measure nitrate every 10 minutes. The ISUS worked well for the first day of deployment but soon failed to give correct values when the average spectral level dropped too low. We noticed rust stains on the probe tip and optical window. Manual cleaning helped a little, but the ISUS soon gave bad values again. It was sent to the manufacturer who replaced the probe tip and optical window. We added the sequence of 50- and 1- $\mu\text{m}$  filters as mentioned in the Problems subsection above to remove the rust in early April 2005. This solved the visible rust-staining problem, but the ISUS only operated correctly from 10 April to 4 May 2005 and then sporadically immediately after cleaning cycles. Following a presentation ((Cokelet, E. D., Jenkins, A. J., Pegau, W. S., Mordy, C. W., and Sullivan, M. E., 2005)) on the *Tustumena* system at the 2005 ASLO Summer Meeting, Friedhelm Schroeder of the GKSS Institute for Coastal Research, Germany, suggested that we clean the optical window with a cotton swab and oxalic acid (Schroeder, F. and Koch, M., 2005). We tried that on 19 July 2005, and the ISUS immediately began reporting realistic data. Commencing then, we added oxalic acid probe-tip cleaning to our routine maintenance protocol. Apparently an organic-iron-oxide film was forming on the probe tip. It was transparent to visible light, but opaque to ultraviolet light. Oxalic acid removed this film.

On calibration cruises, water samples were collected, frozen and sent to PMEL for nitrate analysis. Samples were collected in acid-cleaned 40 ml HDPE Boston Round sample bottles, triple rinsed from the underway seawater line. To prevent loss of sample due to expansion when freezing, a 1-2 cm air gap was left at the top of the sample bottle and samples were frozen in an upright position (Dore, J., Houlihan, T., Hebel, D., Tien, G., Tupas, L., and Karl, D., 1996). The majority of samples were analyzed at PMEL within 8 months, but some samples were analyzed 11 months after collection. Samples were thawed in a cool water bath and immediately analyzed. Nitrate and nitrite analyses were modified from Armstrong et al. (1967). Nitrate was reduced to nitrite in a cadmium column, and formed into a red azo dye by complexing nitrite with sulfanilamide and N-1-naphthylethylenediamine. The color formation of the dye was dependent on the concentration of nitrite, and was detected at 540 nm through a 10 mm flow cell. Because this technique measures nitrate plus nitrite, a second channel was used to measure only nitrite in the sample (the same technique was used without the reduction step), and nitrate was determined by difference. Nitrate and nitrite were measured using automated continuous flow analysis with a segmented flow and colorimetric detection. The two-channel autoanalyzer was customized using components from various systems. The major components were an Alpkem 301 sampler, a 24 channel Ismatek peristaltic pump, micro-coils and glass tubing from Irama Corp., two spectrophotometers from Fox Scientific, and custom software for digitally logging and processing the chromatographs. Standardization and analysis procedures specified by Gordon et al. (1994) were closely

followed including calibration of lab ware, preparation of primary and secondary standards, and corrections for blanks and refractive index. Discrete nitrate determinations were precise to within 0.2  $\mu\text{M}$  and accurate to better than 0.5  $\mu\text{M}$ .

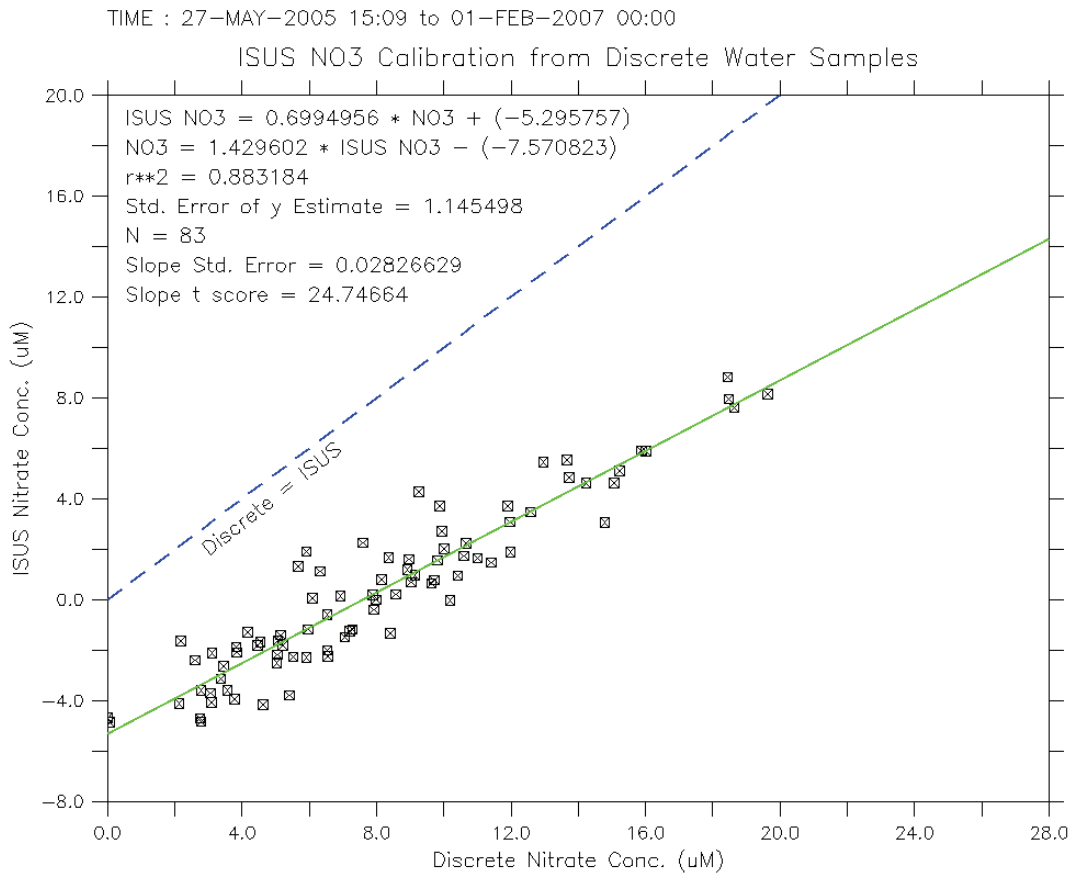


Figure 7. ISUS nitrate calibration from discrete water bottle samples before the shutter-dust fouling problem was discovered. Black symbols represent the data points, the green line is the linear least squares fit, and the dashed blue line represents the line along which the data points would lie if the samples from the two sources matched exactly.

A linear least-squares fit of the ISUS values versus concurrent analyzed discrete nitrate samples gave the calibration curve shown in Figure 7. It applies to the time period between the first probe-tip replacement in March 2005 and the next ISUS factory maintenance in February 2007. The fit accounted for 88% of the variance with a standard error of 1.15  $\mu\text{M}$ . Compared to the discrete samples, the ISUS values were biased low by 5 to 10  $\mu\text{M}$ . The inverse fit equation,  $\text{NO}_3 = 1.43 \text{NO}_{3:\text{ISUS}} + 7.57$ , was used to calibrate the ISUS values for this time period. At the February 2007 factory inspection, Satlantic found that dust from the plastic shutter within the instrument had coated the lens contributing to low spectral levels. The shutter was replaced, cycled several times to seat

properly and the lens cleaned. This newly discovered shutter-dust problem led the manufacturer to apply this break-in procedure to future ISUS factory inspections. Following the shutter-dust cleaning, the ISUS calibration changed dramatically as shown by the least-squares fit in Figure 8 that covers the February 2007 to October 2008 period. During this period in February 2008, the instrument was factory-checked and calibrated, but its field calibration did not change appreciably. As Figure 8 shows, the second linear least squares fit ( $\text{NO}_3 = 1.30 \text{NO}_{3:\text{ISUS}} - 2.07$ ) accounted for the same amount of variance (88%) with a similar standard error ( $1.29 \mu\text{M}$ ) as before, but now the ISUS nitrate values bracketed the discrete calibration values along the blue dashed line of equality. Earlier, shutter dust on the lens had biased the ISUS nitrate values low. The results show that with field calibration, the ISUS nitrate is accurate to within  $1.3 \mu\text{M}$  as compared to an accuracy of  $0.5 \mu\text{M}$  for laboratory-analyzed discrete samples. Periodic probe-tip cleaning with oxalic acid was still required, even in the absence of shutter dust.

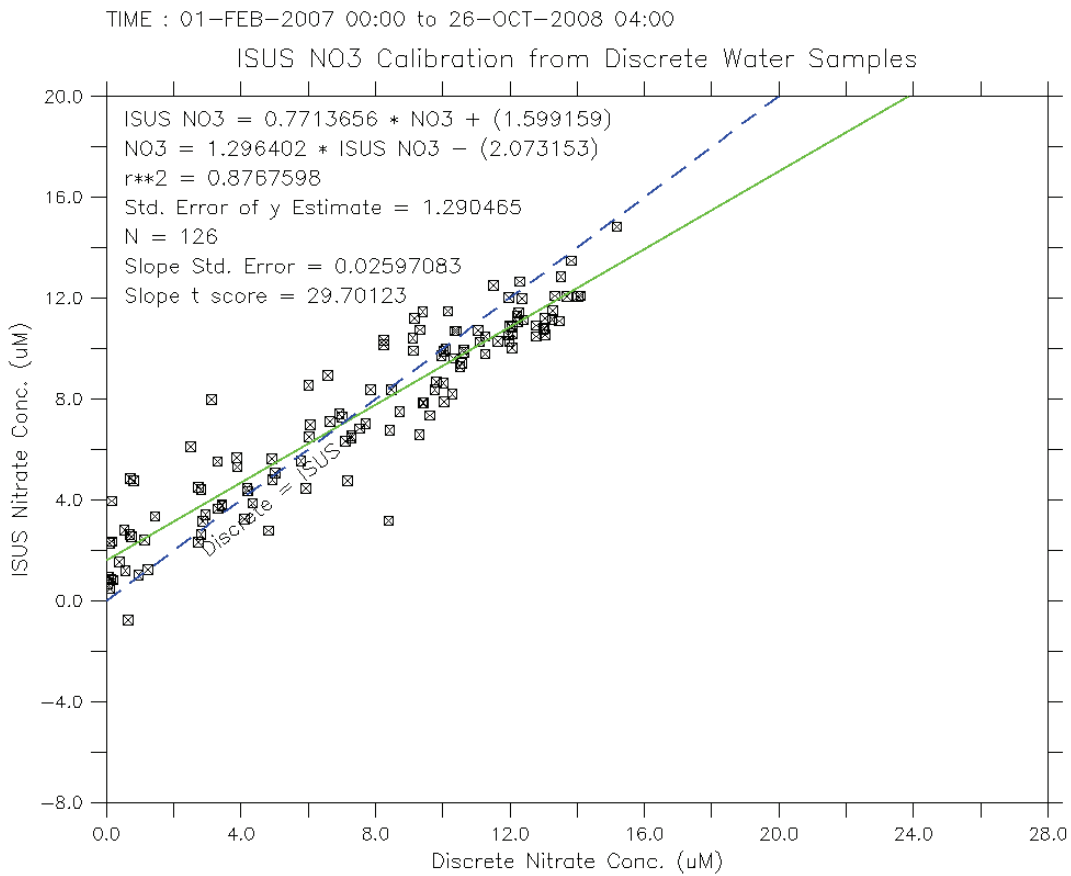


Figure 8. ISUS nitrate calibration from discrete water bottle samples after the shutter-dust fouling problem was rectified. Black symbols represent the data points, the green line is the linear least squares fit, and the dashed blue line represents the line along which the data points would lie if the samples from the two sources matched exactly.

Chlorophyll fluorescence, a proxy for phytoplankton chlorophyll concentration, was measured with fluorometers (Table 1) tuned to the chlorophyll excitation (470 nm) and emission wavelengths (695 nm). A WET Labs WETStar chlorophyll fluorometer was used during 2005. Although this instrument was designed for flow-through applications, it was not self-cleaning and would often foul between manual cleanings in Homer. A WET Labs ECO fluorometer with a bio-wiper that cleaned automatically was used in 2006-2008. This instrument was designed for CTD applications. We built a 15-cm diameter, 14-cm long cylindrical flow-through cell and installed the ECO fluorometer in it with the fluorometer face flush with the inside of one end. Each fluorometer was calibrated against discrete chlorophyll samples taken on calibration cruises. Calibration samples were collected in 60 or 100-ml plastic sample bottles, triple rinsed from the underway seawater line. The water was filtered through 0.7- $\mu\text{m}$  pore size glass fiber

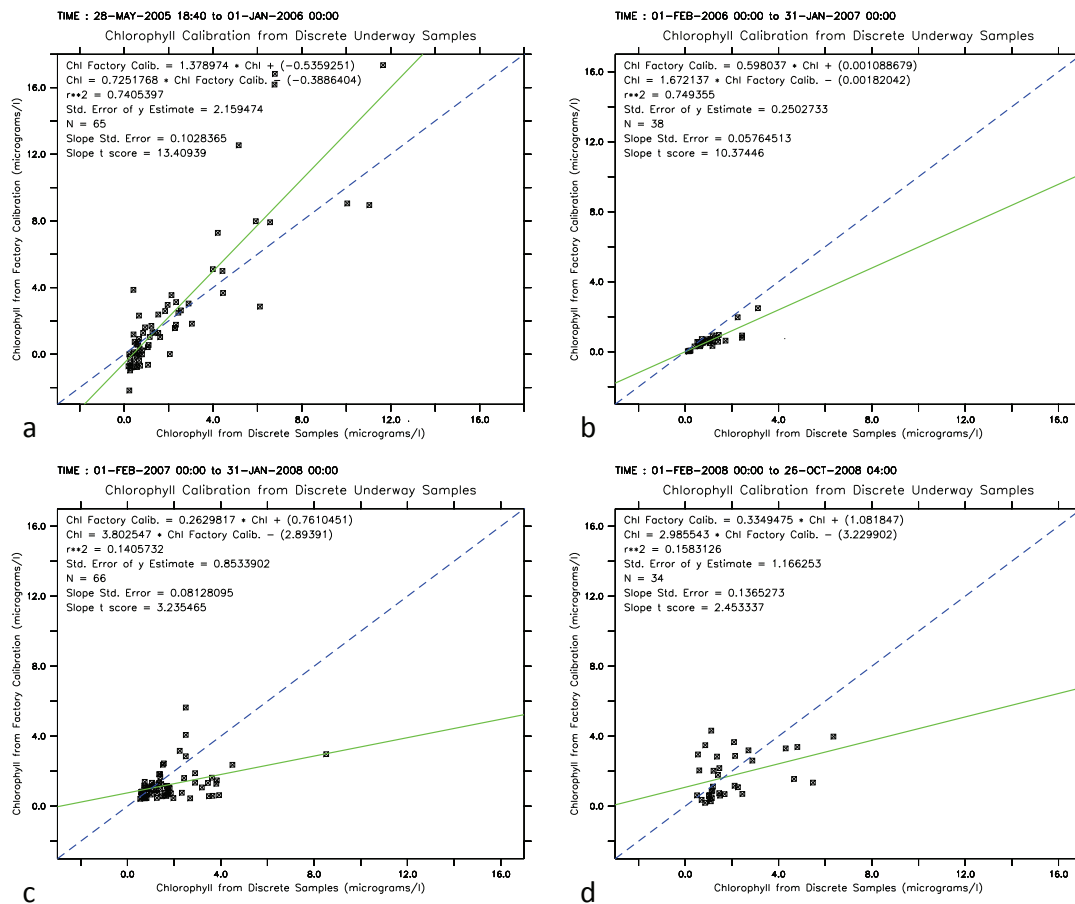


Figure 9. Fluorometer chlorophyll calibrations from discrete water samples for (a) the WETStar in 2005, and the ECO fluorometers in (b) 2006, (c) 2007 and (d) 2008. Black symbols represent the data points, the green line is the linear least squares fit, and the dashed blue line represents the line along which the data points would lie if the samples from the two sources matched exactly.

filters. The filters were placed in labeled microcentrifuge tubes and briefly frozen on the ship at  $-13^{\circ}\text{C}$  for later laboratory analysis. On land they were transferred to a  $-80^{\circ}\text{C}$  freezer for several months until extraction in 90% acetone for 24 hours. The fluorometric determination of chlorophyll concentration via the acidification method (Lorenzen, C., 1966) was made in the laboratory using a Turner Designs TD700 fluorometer calibrated with pure chlorophyll a. Based upon factory calibrations using a marine diatom (*Thalassiosira weissflogii*) as a standard (WET Labs, 2004), the WET Labs instruments' fluorescence voltages,  $Fl_{\text{chl}}$ , were related to the chlorophyll concentration,  $\text{Chl}_{\text{FI}}$  via the factory-calibrated scale factor,  $SF_{\text{chl}}$ , and dark voltage,  $V_{\text{ref}}$ , by the following formula:  $\text{Chl}_{\text{FI}} = SF_{\text{chl}} (Fl_{\text{chl}} - V_{\text{ref}})$ . For each deployment year, we computed a linear least squares fit of the factory-calibrated chlorophyll versus the discrete sample concentration from calibration cruises as shown in Figure 9. For the 2005, 2006, 2007 and 2008 deployments the standard errors of the fits were 2.16, 0.25, 0.85 and 1.17  $\mu\text{g/l}$ . Student's t-tests showed that each of the linear slopes was significantly different from zero with greater than 98% confidence, confirming the relationship between fluorescence and chlorophyll concentration. Also in no case did the 95% confidence limits of the slope encompass a line of slope 1, implying that the marine diatom fluorescence-chlorophyll relationship used by the factory did not represent the phytoplankton conditions that we encountered in the field. The 2005 WETStar and the 2006 ECO fluorometer fits were good, accounting for 74% and 75% of the variance. However the 2007 and 2008 ECO fluorometer fits were more scattered, accounting for only 14% and 16% of the variance. Unfortunately the calibration cruises sampled low chlorophyll concentrations ( $< 8 \mu\text{g/l}$ ) each year after 2005. Based upon the factory calibrations, the WETStar overestimated the chlorophyll concentration on average, whereas the ECO fluorometers underestimated it. The conversion of chlorophyll fluorescence measured from a moving ship to chlorophyll concentration is an imprecise process because the relationship depends upon the phytoplankton species, the condition of the cells, and their history of light exposure – all of which depend upon location and time.

Colored dissolved organic matter (CDOM, aka yellow substance) fluorescence was measured with fluorometers (Table 1) tuned to the CDOM excitation (370 nm) and emission wavelengths (460 nm). A WET Labs WETStar CDOM fluorometer requiring periodic cleaning was used until 30 July 2006 followed by a WET Labs ECO fluorometer with a bio-wiper that cleaned automatically. No discrete oceanic calibration samples were acquired. According to the manufacturer's manual (WET Labs, 2004), the CDOM concentration in quinine sulfate dihydrate equivalence (ppb) is related to the fluorescence voltage output,  $Fl_{\text{CDOM}}$ , the factory calibrated scale factor,  $SF_{\text{CDOM}}$ , and the instrument clean water offset,  $CWO_{\text{CDOM}}$ , by the following formula:  $\text{CDOM} = SF_{\text{CDOM}} (Fl_{\text{CDOM}} - CWO_{\text{CDOM}})$ . Factory calibrations in March 2003, December 2004, July 2006, February 2007 and February 2008 provided values of  $SF_{\text{CDOM}}$  and  $CWO_{\text{CDOM}}$  that were used to convert the measured fluorescence voltage to CDOM concentration. In the end, the CDOM data from 2004-2006 were rejected because they were too noisy and contained unexplainable baseline shifts compared to the 2007 and 2008 data.

Optical collimated beam attenuation over a 25-cm path length was measured with a WET Labs C-Star transmissometer at a wavelength of 660 nm, appropriate for measuring the light loss due to particle scattering. No discrete oceanic calibration samples were acquired to calibrate the transmissometer. According to the manufacturer's manual (WET Labs, 2003), the transmittance,  $Tr$ , is related to the voltage output by the following formula:  $Tr = (V - V_{\text{dark}})/(V_{\text{ref}} - V_{\text{dark}})$  where  $V$  is the output voltage,  $V_{\text{dark}}$  is the meter output when the light path is blocked and  $V_{\text{ref}}$  is the meter output in clean water. Factory calibrations in November 2003, December 2004, June 2005, February 2007 and March 2008 provided values of  $V_{\text{dark}}$  and  $V_{\text{ref}}$  that were used to convert the measured voltage to transmittance. Periods when  $Tr$  was near zero and the transmissometer was not working properly were excluded from the data set. The transmittance is related to the attenuation coefficient,  $c$  an inherent optical property of the water, by the following formula

$$Tr = e^{-cx} \quad (2)$$

where  $x$  is the path length of the light. Unfortunately the transmissometer employed no

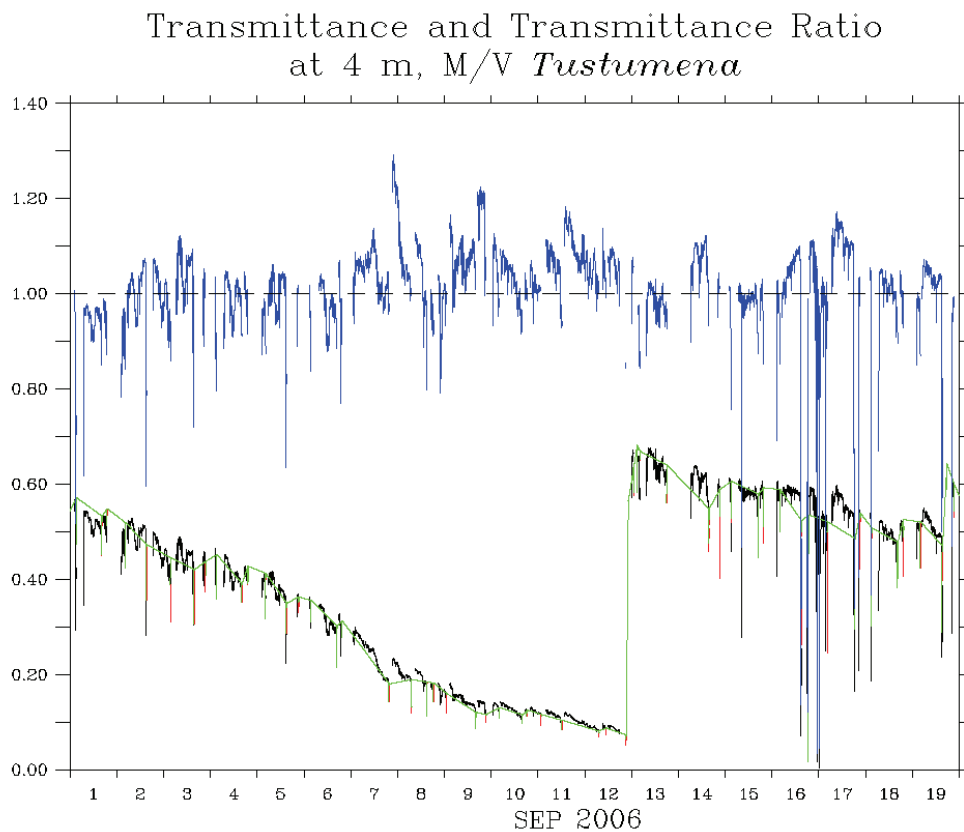


Figure 10. Time series of the optical beam transmittance,  $Tr$ , of ocean water (black curve), fresh water during backflashes (red curve) and the maximum fresh-water backflush values,  $Tr_{\text{fw}}$  (green curve) during September 2006. Also shown is the ratio of the ocean to fresh water transmittance (blue curve).

self-cleaning mechanism, and its light level was a function of both the sediment load and the cleanliness of the optics. Therefore no direct inference could be made about the distribution of suspended sediment over the ferry's route. Figure 10 is a typical example of how the transmittance (black curve) fluctuated along the route but also steadily decreased due to fouling, until it rebounded on 13 September when the instrument was cleaned by hand. Besides the seawater measurements, the transmissometer also ran during the automatic fresh-water backflushes that were performed during each port call, or whenever the control system (Appendix) sensed a need to backflush. The intermittent red curve in Figure 10 shows that the backflush transmittance behaved like the seawater curve, decreasing between manual cleanings. The backflush transmittance can be used as a reference value to remove the effects of fouling if one assumes that the potable fresh water had a relatively low and consistent particulate concentration. The green curve in Figure 10 links the maximum fresh-water backflush transmittance values. The blue curve is the ratio of seawater to maximum fresh-water transmittance,  $Tr/Tr_{fw}$ . Notice how the fouling and subsequent cleaning have no apparent affect on the transmittance ratio around 13 September. This ratio can be related to the attenuation coefficients of oceanic and fresh-water,  $c_{fw}$ , from equation (2) by

$$\frac{Tr}{Tr_{fw}} = e^{-(c-c_{fw})x} \quad (3)$$

which implies

$$c - c_{fw} = -\frac{1}{x} \ln \left( \frac{Tr}{Tr_{fw}} \right). \quad (4)$$

Therefore the effect of forming the ratio of the two transmittances is equivalent to differencing the attenuation coefficients of oceanic and fresh water. The effect of fouling on the two attenuation coefficients measured simultaneously will be removed by the subtraction.

## **Results:**

The sea surface temperature (SST) is a basic physical property of the marine ecosystem, but it can take many forms. The Group for High Resolution SST (GHRSSST) has proposed a theoretical framework to define the SST at several levels in the upper layer of the ocean (GHRSSST-PP SST Science Team, 2010). At the air-sea interface within the upper few microns is the theoretical, but currently impossible-to-measure, interface temperature. Below that are the skin and sub-skin temperatures typically measured by microwave remote sensing devices at depths of tens of microns. Still deeper at centimeters to meters is the SST at depth ( $SST_z$ ) as measured by thermal contact devices such as buoys, thermistor chains, profiling instruments and shipboard systems. A fundamental concept is the foundation temperature,  $SST_{\text{fnd}}$ , defined as the temperature of the water column free of diurnal temperature variability due to radiation, which could be at a depth of 1 to 20+ m depending on solar radiation and mixing conditions. That is below where daytime heating and nighttime cooling affect the water temperature under light winds. *Tustumena* measured the sea chest intake temperature at 4 m or  $SST_4$  by the GHRSSST definition. Owing to the propensity for low solar radiation due to clouds and to strong tidal currents and winds in the coastal Gulf of Alaska, the upper ocean is often well mixed and  $SST_4 \approx SST_{\text{fnd}}$ .

Figure 11 depicts the time series of the sea chest intake temperature measured over the entire ferry route. The seasonal cycle from warm in summer to cold in winter is apparent. *Tustumena* spent most of its time on the Homer-Kodiak route, with trips into Prince William Sound in 2005 and to Dutch Harbor each summer (Figure 2). As the graph shows, the measurement period was weighted toward summer months owing to wintertime shipyard repairs and equipment downtime. High-frequency variations (red line in Figure 11) about the 30-day running mean (blue curve) come from spatial differences along the track. The temperature extremes occurred in sheltered harbors where ice might form in winter, and thin layers stratified by glacial melt water formed in summer. The temperature ranged between  $-1.60^\circ\text{C}$ , in Kachemak Bay near Homer on 2 March 2007, and  $17.00^\circ\text{C}$ , in Resurrection Bay near Seward on 15 July 2005, with an overall mean of  $7.86^\circ\text{C}$ . The map in Figure 12 shows how the temperature varied along-track during July 2005 with the warmest water in Resurrection Bay and the coldest in Marmot Strait, between the Barren Islands and at the southwestern tip of the Kenai Peninsula. Colder water was often encountered in Marmot Strait and the Barren Islands due to deep water being mixed up by strong tidal currents in these narrow passes.

*Tustumena* Intake Temperature at 4 m

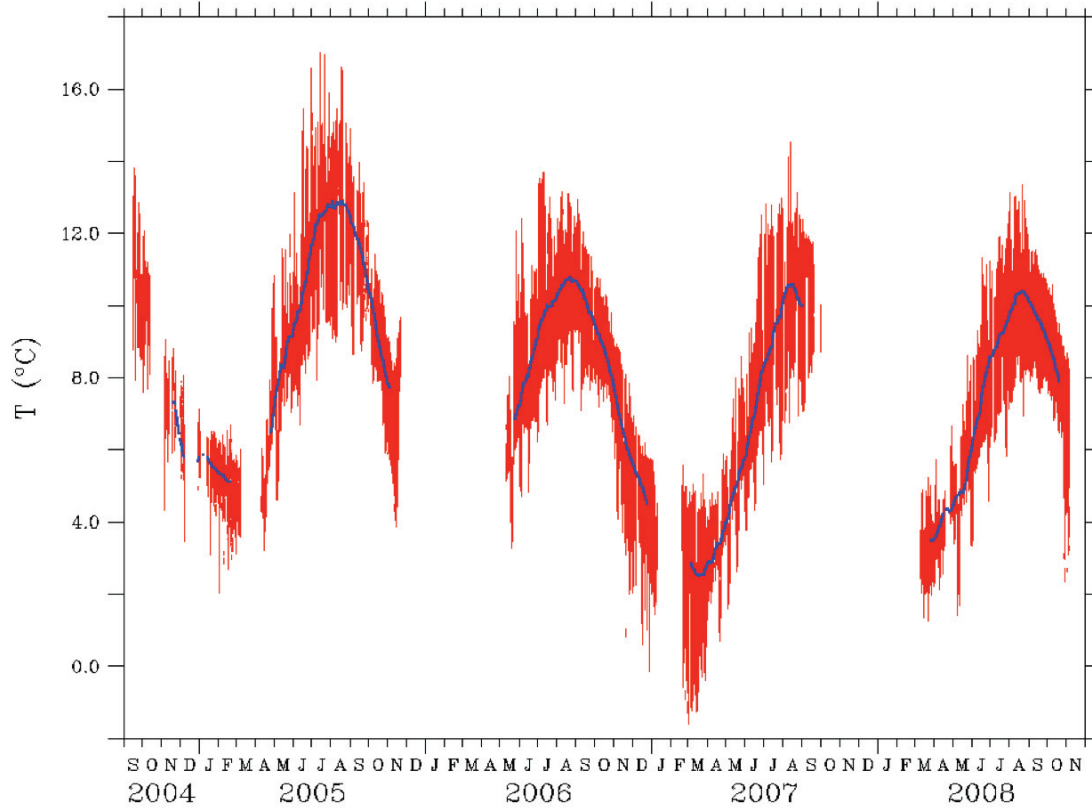


Figure 11. Time series of *Tustumena*'s sea chest intake temperature at 4 m depth. The smooth blue curve represents a 30-day running mean of the observations.

Temperature at 4 m, M/V *Tustumena*  
 12-JUL-2005 15:39:00 to 14-JUL-2005 23:51:00 GMT

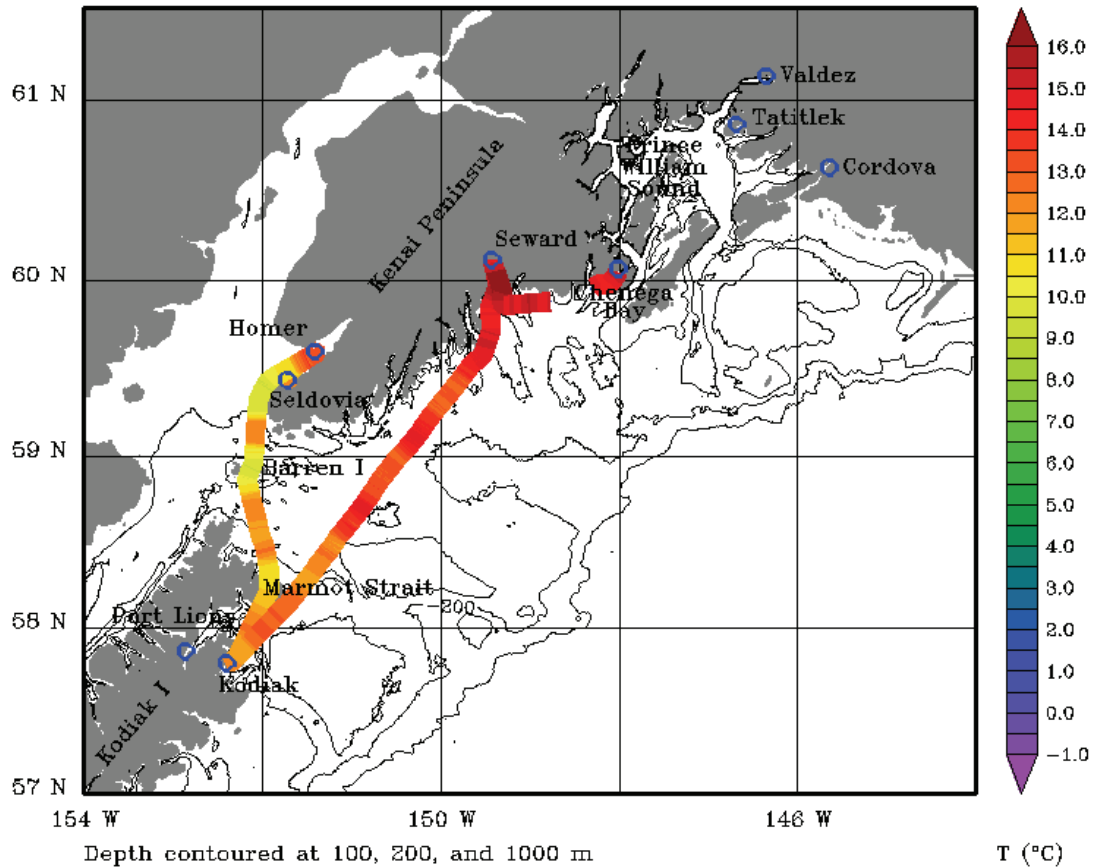


Figure 12. Map of the water temperature along *Tustumena*'s route on 12-14 July 2005.

The salinity time series over the entire observation period is shown in Figure 13. The salinity varied more along the ferry route than it did between seasons, but generally the salinity was lowest in the late summer during high ice melt and runoff conditions and highest in the winter when water was sequestered on land as snow and ice. The salinity ranged between 6.44 and 33.00 psu with an overall mean of 31.17 psu. The freshest water was encountered in Resurrection Bay on 4 October 2004 and the saltiest in Unimak Pass on 21 May 2006. The sharp salinity dips occurred when the ship entered an estuarine port such as Seward in Resurrection Bay or Homer in Kachemak Bay. The salinity map in Figure 14 illustrates this behavior. This map corresponds to the same time span as the temperature map of Figure 12. Often higher salinities occurred in Marmot Strait and the Barren Islands corresponding to the colder water brought up by mixing.

*Tustumena* Salinity at 4 m

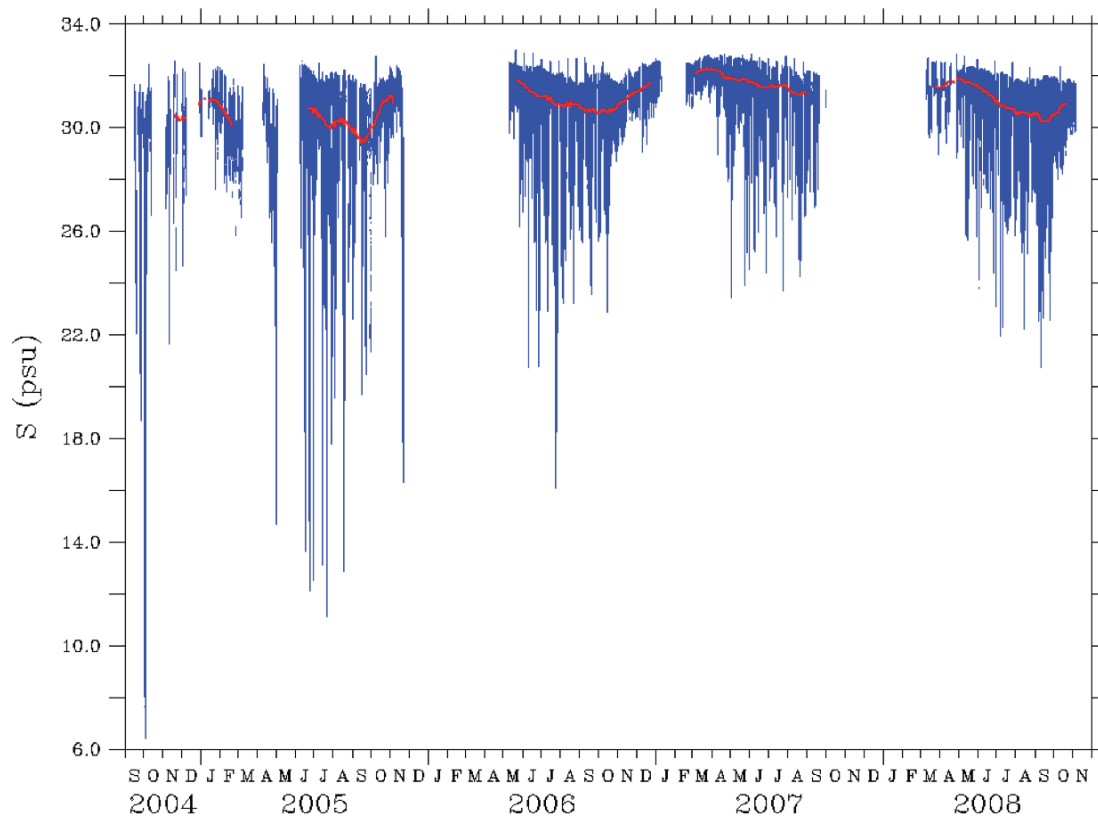


Figure 13. Time series of *Tustumena*'s salinity at 4 m depth. The smooth red curve represents a 30-day running mean of the observations.

Salinity at 4 m, M/V *Tustumena*  
 12-JUL-2005 15:39:00 to 14-JUL-2005 23:51:00 GMT

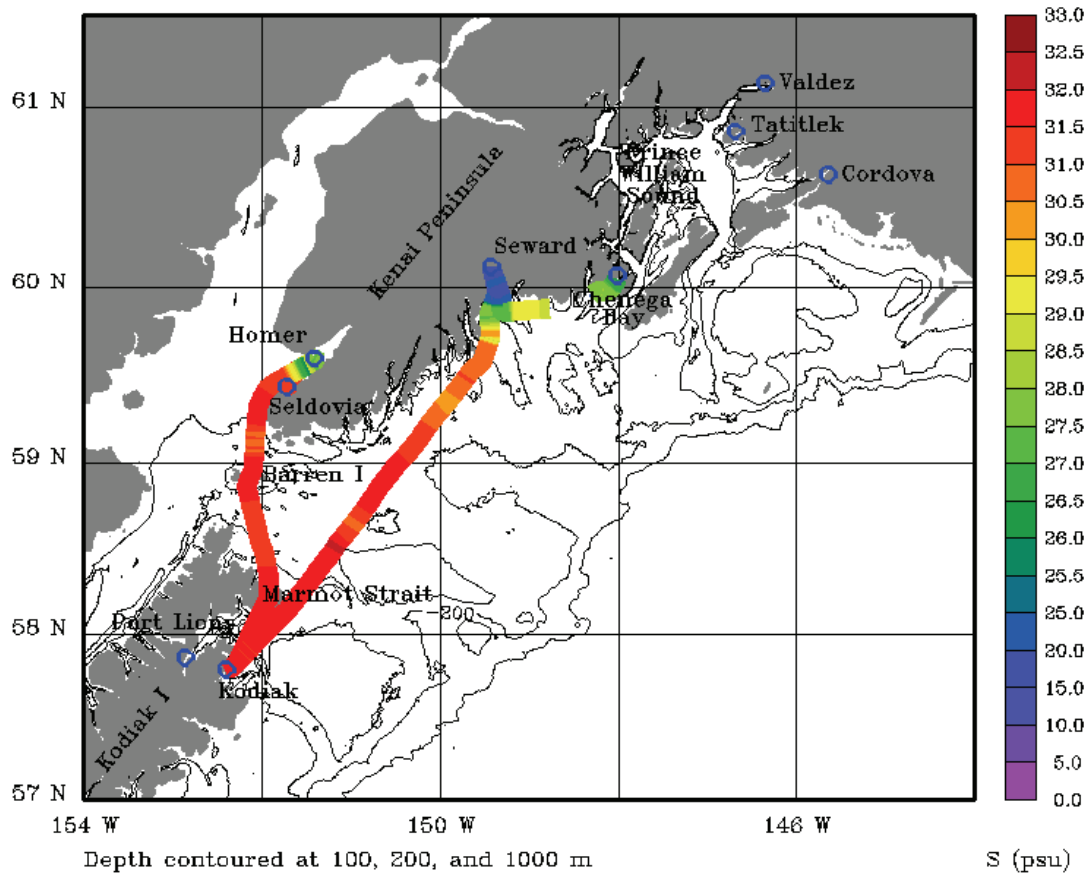


Figure 14. Map of the salinity along *Tustumena*'s route on 12-14 July 2005.

A comparison of the temperature and salinity measurements with an independent source gives confidence in the observations. The University of Alaska Fairbanks maintains a data set of a sequence of oceanographic CTD casts taken at the GAK1 site along the Seward Line in the Gulf of Alaska dating from December 1970 to the present (Weingartner, T., Danielson, S. L., and Leech, D., 2010). Between 1 September 2004 and 1 October 2005, *Tustumena* passed within a 3 x 3 km box centered on the GAK1 site (59.85°N, 149.47°W) a total of 71 times. For each transit through the box, we extracted the mean underway temperature and salinity and compared it to the CTD cast values at the surface. Figure 15 shows the comparison between the temperatures measured by the CTD casts

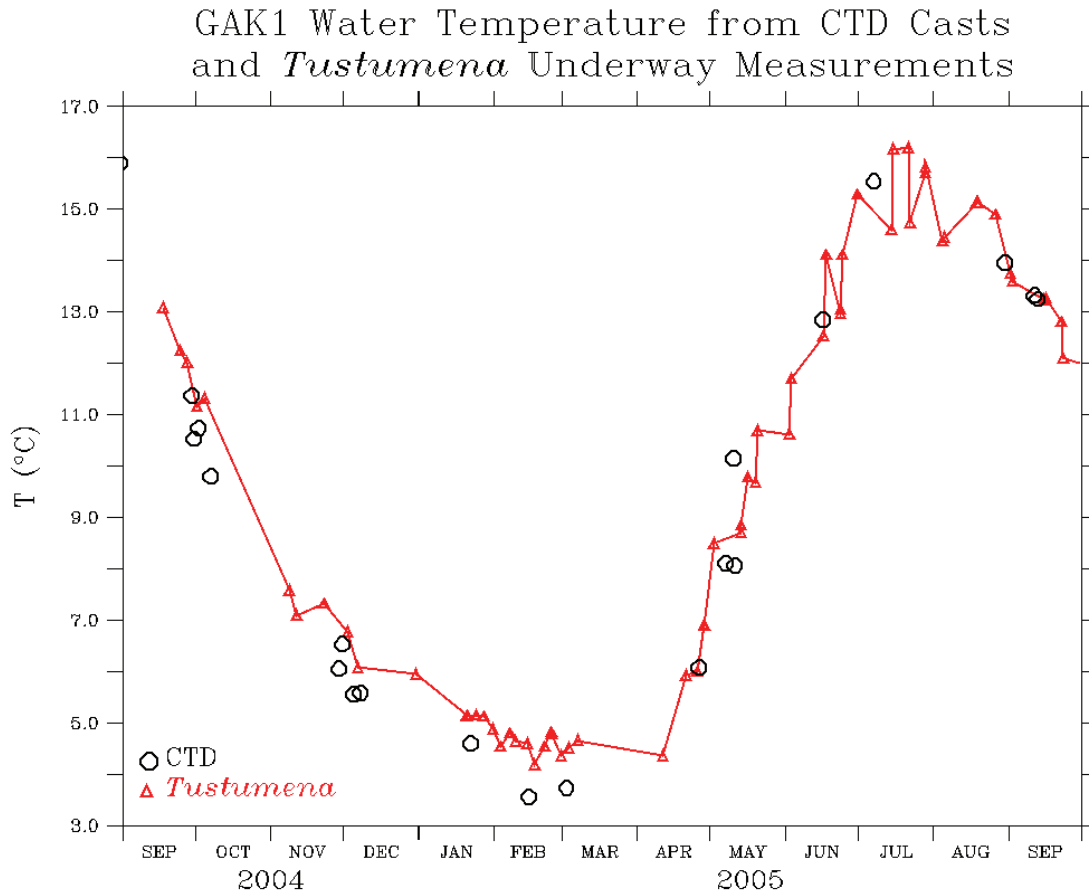


Figure 15. The near-surface temperature measured at GAK1 from CTD measurements and *Tustumena*'s underway system.

and *Tustumena*'s underway system. Both measurements are in general agreement and show the annual temperature cycle reaching a minimum in February and a maximum in July. A direct comparison is not possible because the measurements do not coincide. However a comparison between the CTD temperature and the underway temperature linearly interpolated to the CTD cast times shows the ship temperature exceeded the CTD temperature by 0.34°C on average. This difference could be due to the temporal variability in the water temperature and the error associated with linear interpolation, to the heating of the water as it entered the ship or to a combination of the two. Figure 16 shows a similar comparison between the CTD and *Tustumena* salinity. When the observations are confined to one location instead of the entire region as in Figure 13, the annual salinity cycle is more apparent. The ship's salinity, linearly interpolated to the CTD cast times, was on average 0.017 psu higher than the CTD values, which is small compared to the natural variability. The error bars in Figure 16 represent  $\pm$  one

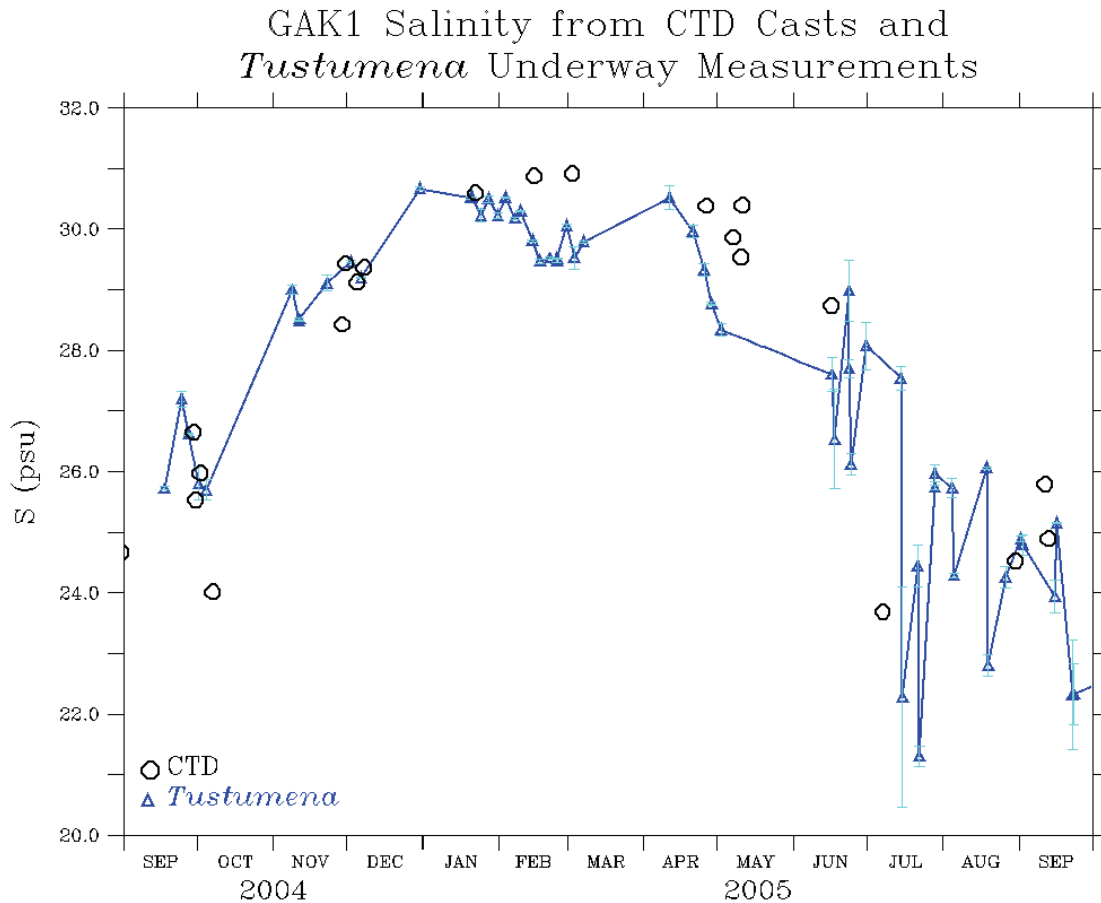


Figure 16. The near-surface salinity measured at GAK1 from CTD measurements and *Tustumena*'s underway system. Error bars are  $\pm$  one standard deviation about the mean salinity values obtained during each passage through the 3 x 3 km box centered on GAK1.

standard deviation about the mean salinity values obtained during each ship passage through the 3 x 3 km box centered on GAK1. The ship spent about 5-7 minutes within the box sampling every 30 seconds. Similar temperature error bars are not shown in Figure 15 because they are too small to be discerned. The salinity observations have more scatter due to along-track variations of fresh water encountered as the ship sailed past rivers and glaciers in Resurrection Bay. Figure 17 shows maps of the temperature and salinity during ferry runs to and from Seward on 16-17 June 2005. The GAK1 CTD site is in the southwestern corner, slightly west of the ferry route. Tidal currents advect the strong salinity gradient back and forth across GAK1, leading to salinity variability.

Temperature and Salinity Measured by *Tustumena* in Resurrection Bay  
16-17 June 2005

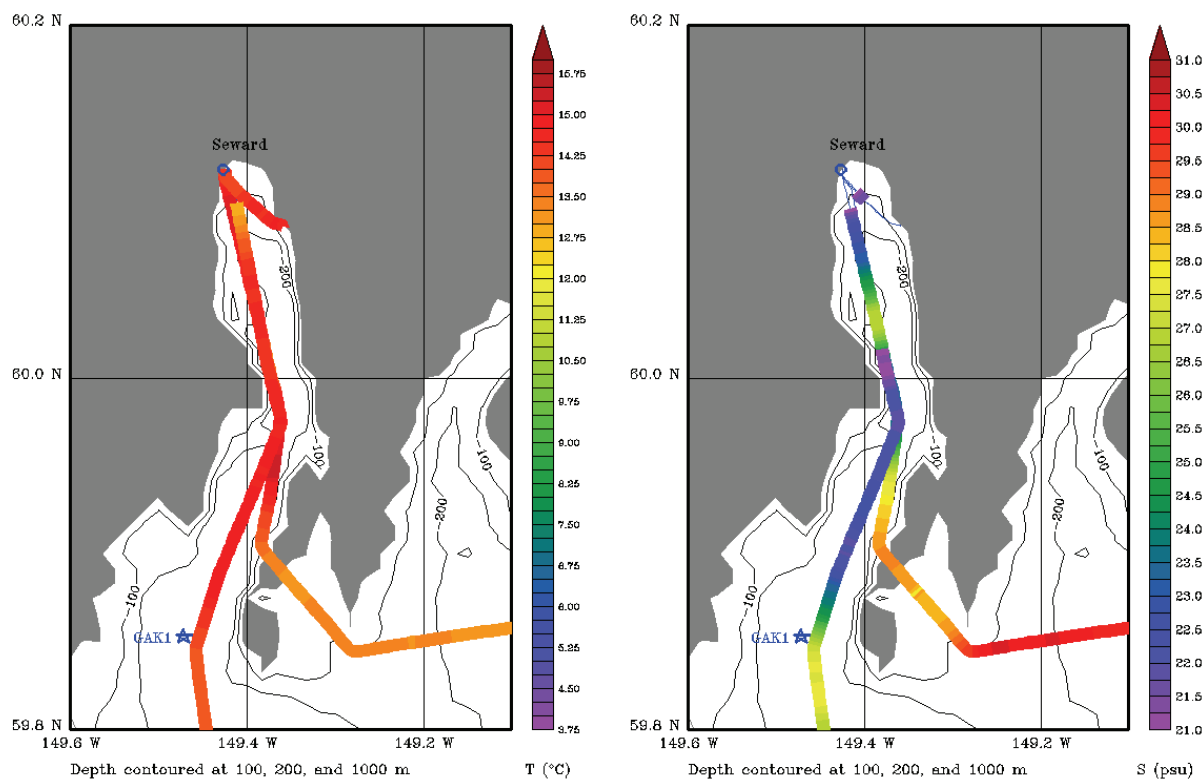


Figure 17. Temperature and salinity measured in Resurrection Bay from *Tustumena* on 16-17 June 2005 showing the location of the GAK1 CTD site relative to the ship track.

The measurement of dissolved nitrate on an underway-oceanographic system was new to the Gulf of Alaska. Results indicate that nitrate varied markedly along the ship track and through the seasons (Figure 18). Nitrate was lowest during the spring and summer phytoplankton growing seasons when it was utilized for photosynthetic production. Conversely it was highest in winter when sunlight and phytoplankton growth were reduced and storm-induced mixing brought nutrient-rich water up from depth. The highest concentration ( $37 \mu\text{M}$ ) was measured in November 2005 when the ship transited the Inside Passage to Puget Sound for repairs, but otherwise the maxima in the Gulf of Alaska exceeded  $24 \mu\text{M}$ . The nitrate concentration varied faster along the ship track than with time at a fixed location. Figure 19(a) illustrates how the nitrate concentration ranged from minima in Prince William Sound of  $2\text{--}4 \mu\text{M}$  to maxima in excess of  $24 \mu\text{M}$  over the continental shelf in the Gulf of Alaska during one voyage on 15-17 April 2008.

### *Tustumena* Nitrate Concentration at 4 m

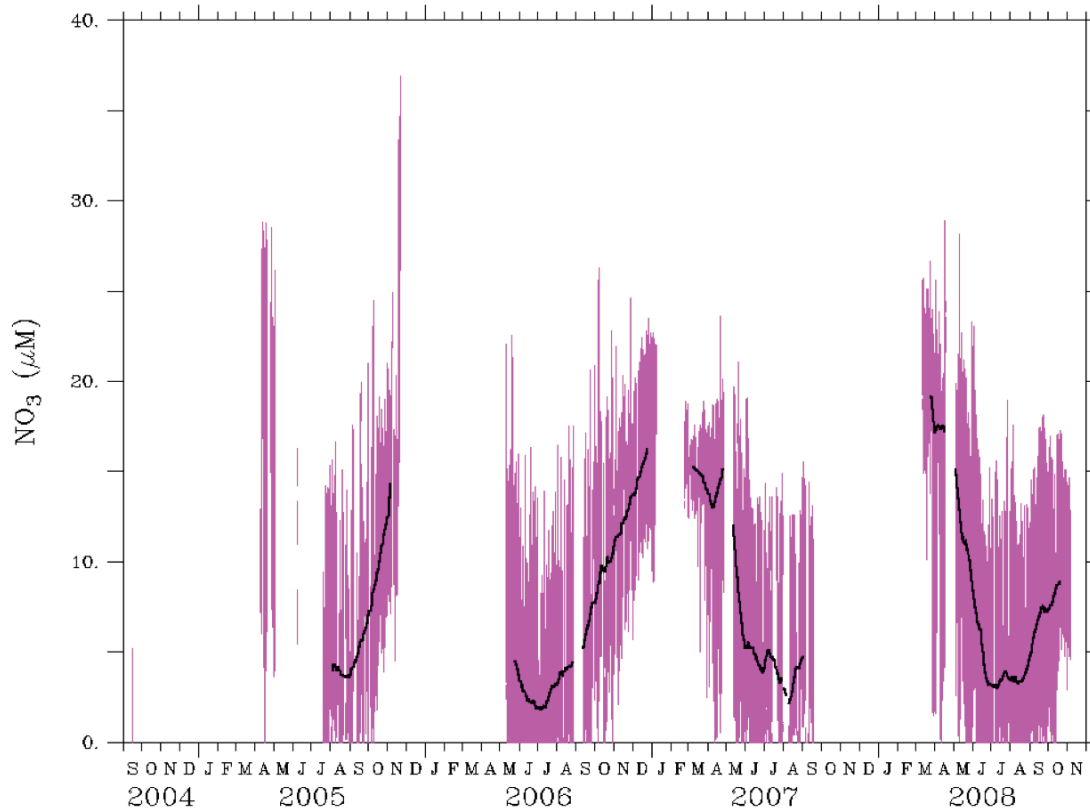


Figure 18. Time series of *Tustumena*'s dissolved nitrate concentration at 4 m depth. The smooth black curve represents a 30-day running mean of the observations.

Figure 20 shows the chlorophyll concentration as a function of time during the *Tustumena* observational period. As with salinity and nitrate, the chlorophyll concentration often varied more rapidly along the ship track with geographical position than it did with time at a fixed site. In general it was low in winter under low sunlight, rose in the spring, peaked in May or June, and decreased through the summer as phytoplankton production consumed the nutrients, and tailed off in autumn with decreasing sunlight. 2007 and 2008 showed higher levels than 2005 and 2006, although late-May-to-early-June observations were unavailable in the earlier two years owing to instrumental problems. The highest chlorophyll concentrations were observed briefly in Prince William Sound, Kachemak Bay, near the city of Kodiak and to the west of Kodiak Island in Shelikof Strait. Figure 19(b) illustrates how the chlorophyll concentration ranged from maxima of over 30  $\mu\text{g}/\text{l}$  in Prince William Sound to near-zero values in the Gulf of Alaska on the same voyage as the nitrate concentration shown in Figure 19(a). Evidently a spring phytoplankton bloom was consuming the nitrate in Prince William Sound, but over the continental shelf the bloom had not yet begun and nitrate values remained high.

# Nitrate and Chlorophyll Concentrations Measured by *Tustumena* 15-17 April 2008

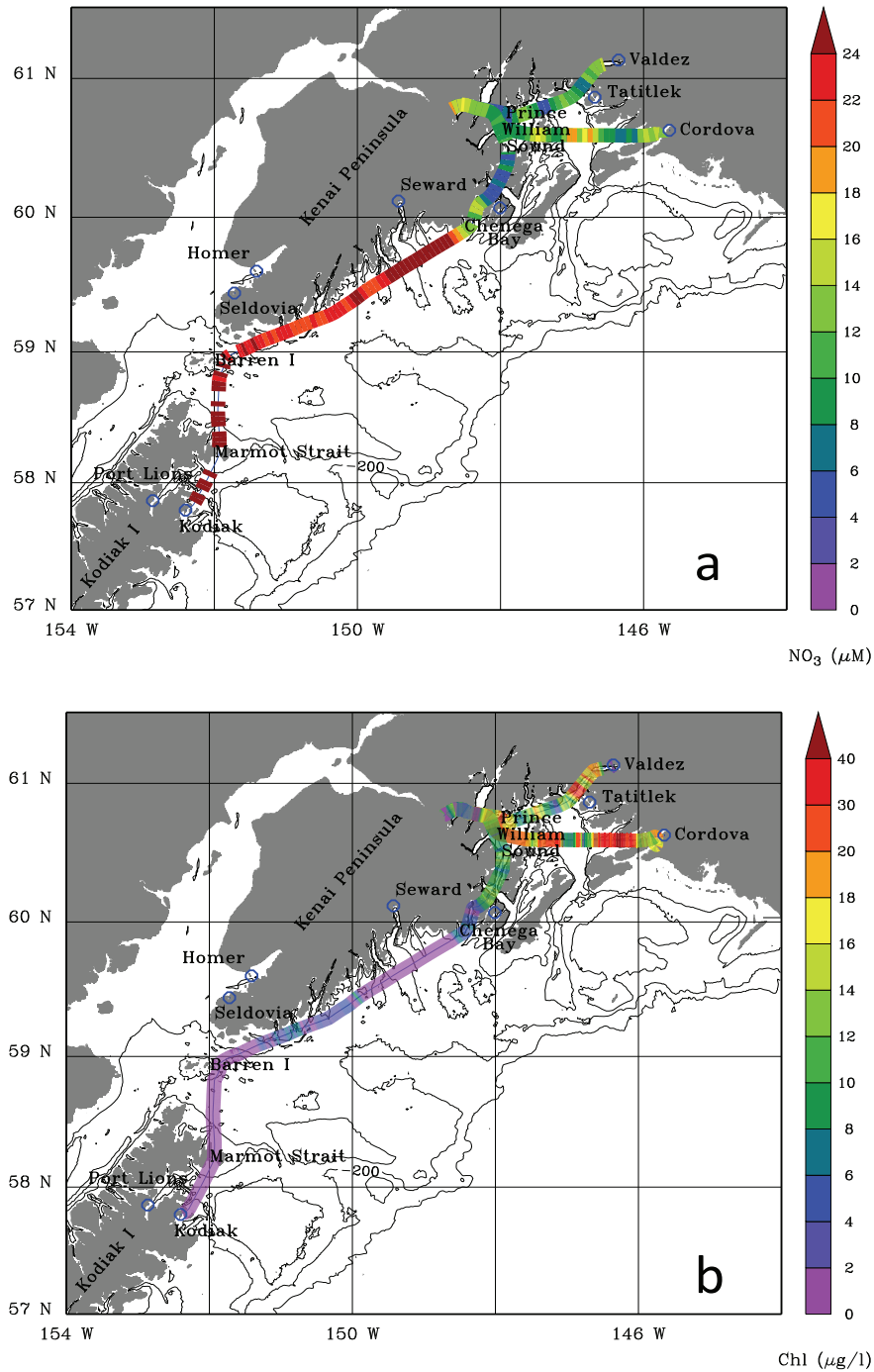


Figure 19. The concentrations of (a) nitrate and (b) chlorophyll along *Tustumena*'s track in the Gulf of Alaska during a trip from Prince William Sound, 15-17 April 2008.

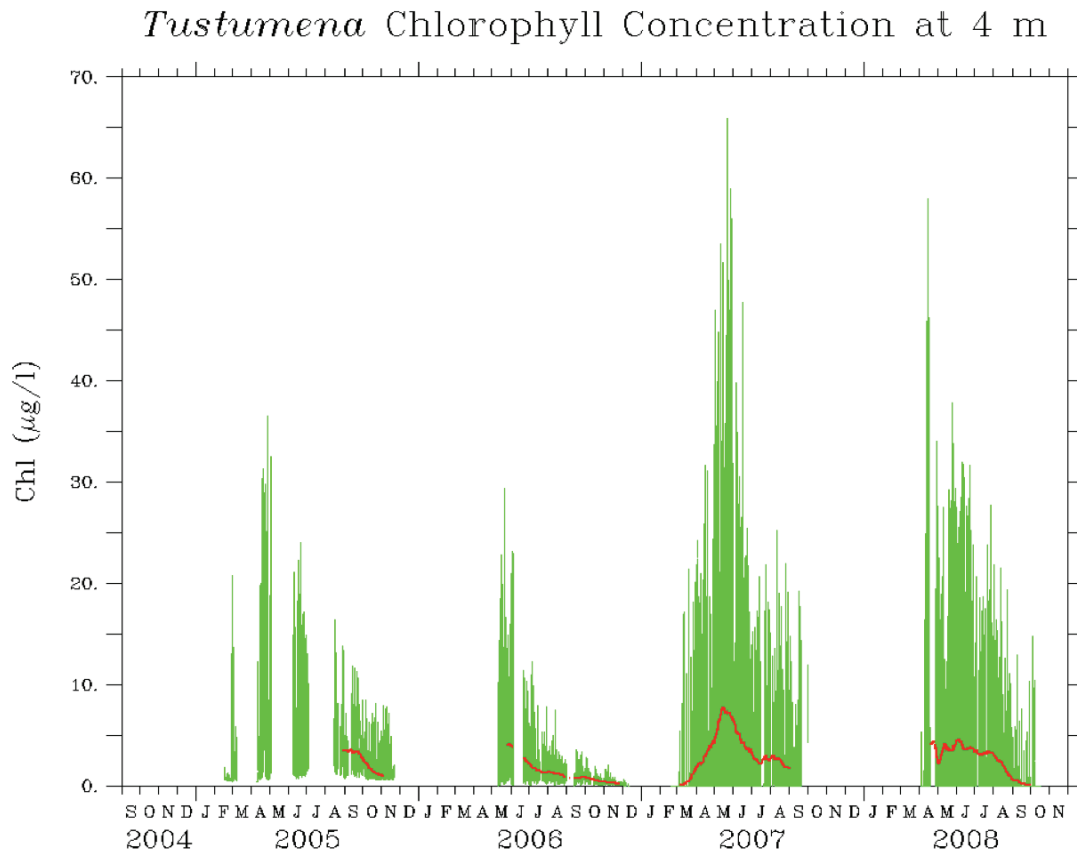


Figure 20. Time series of *Tustumena*'s chlorophyll concentration at 4 m depth. The smooth red curve represents a 30-day running mean of the observations.

The phytoplankton uptake of nitrate to produce biomass leads to a linear relationship between nitrate and chlorophyll (a proxy for phytoplankton biomass). Redfield (1934) showed that for oceanic organisms, the stoichiometric ratio of carbon to nitrogen is 106:16. Therefore on average, phytoplankton will produce 106 moles of organic carbon for every 16 moles of nitrogen they consume via photosynthesis. Our measured chlorophyll concentration can be converted to an inferred carbon concentration based upon a typical carbon-to-chlorophyll mass ratio of 60 as determined empirically for phytoplankton in the Gulf of Alaska (Booth, B. C., Lewin, J., and Lorenzen, C. J., 1988; Frost, B. W., 1993). Given that one mole of carbon weighs 12 g, the inferred carbon mass concentration can be converted to its molar equivalent. Figure 21 shows a scatter plot of inferred carbon versus nitrogen from the *Tustumena* measurements. The nitrogen plotted is from the measured nitrate concentration only, but nitrate accounts for most of the organic nitrogen in the ocean. The observations presented are confined to the spring growth period (March through May) when the interplay between nitrogen and carbon should be most apparent. This excludes winter conditions, when vertical mixing could bring nitrate to surface waters but with no growth owing to light limitation, and post-bloom conditions, when organic matter could sink to deeper water and remineralize. The

linear-least-squares-fit solid line has a negative slope of -2.05 that is significantly different from zero (> 99% confidence), thus verifying the negative linear relationship between carbon and nitrogen. Also shown is a dashed line of negative slope  $106/16 = 6.6$  – the Redfield ratio of C:N – placed so that it passes through the maximum observed nitrate N concentration. It forms a boundary encompassing the vast majority of the 11,240 observations. Why doesn't the best-fit curve slope follow the Redfield ratio? One reason is that the *Tustumena* measurements were made at a constant depth of 4 m, but the upper mixed-layer depth is considerably deeper. Being a dissolved constituent, nitrate has a nearly uniform distribution in the mixed layer, but phytoplankton cells sink toward the pycnocline. Therefore at 4 m there will be a deficit of phytoplankton carbon compared to nitrate that has the effect of lessening the steepness of the best-fit line. The Redfield slope would apply better to measurements averaged over the entire mixed layer where organic carbon production and nitrate consumption are in balance on average. A second reason is that the ferry moves across regions of different initial nitrate concentration at the beginning of the spring bloom. Therefore the bloom starts at different nitrate levels and follows different nitrogen-carbon trajectories leading to the scatter in Figure 21 and lowering the steepness of the best-fit curve of the amalgamated points.

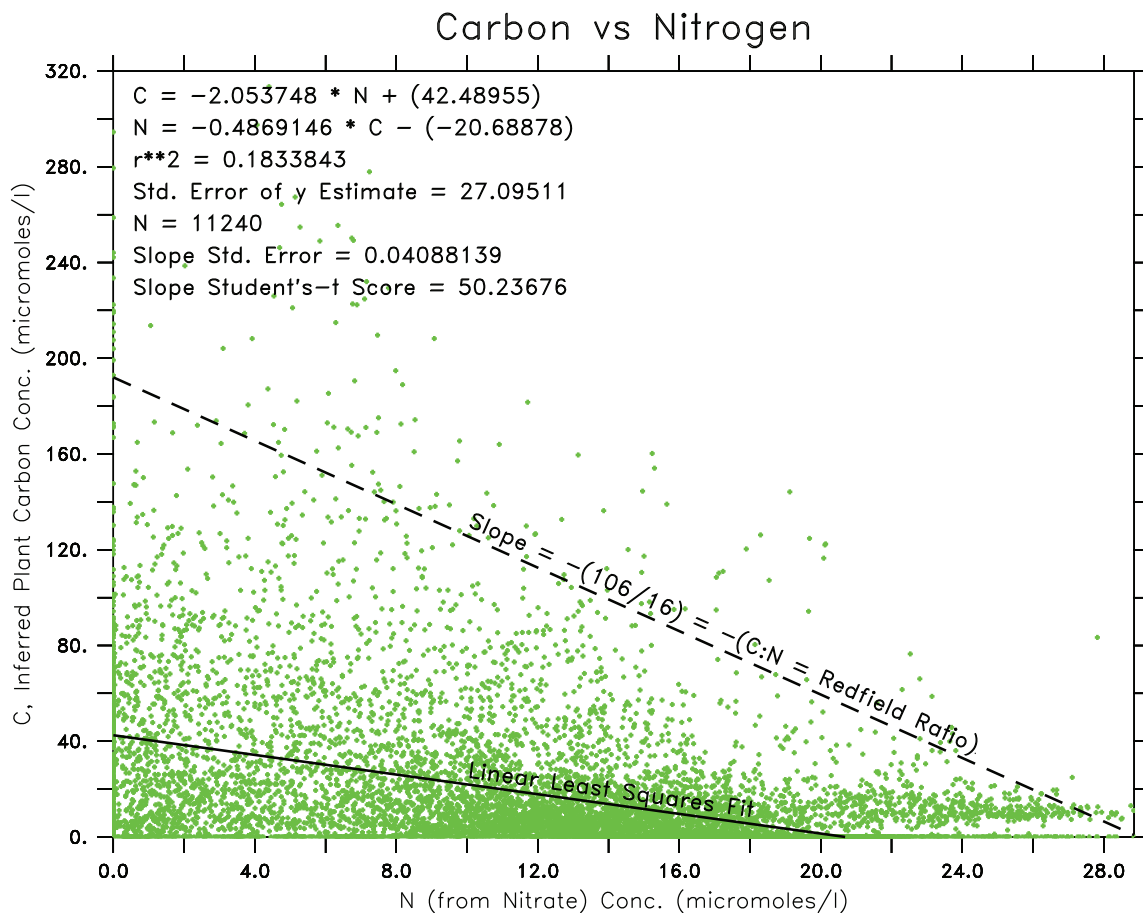


Figure 21. The inferred phytoplankton carbon concentration plotted against the nitrogen (from nitrate) concentration for the March-May 2005-2008 *Tustumena*

measurements. The linear-least-squares fit and Redfield ratio lines are solid and dashed, respectively.

The colored dissolved organic matter time series is shown in Figure 22 for the 2007 and 2008 field seasons. The CDOM fluorometers did not work properly in the early years.

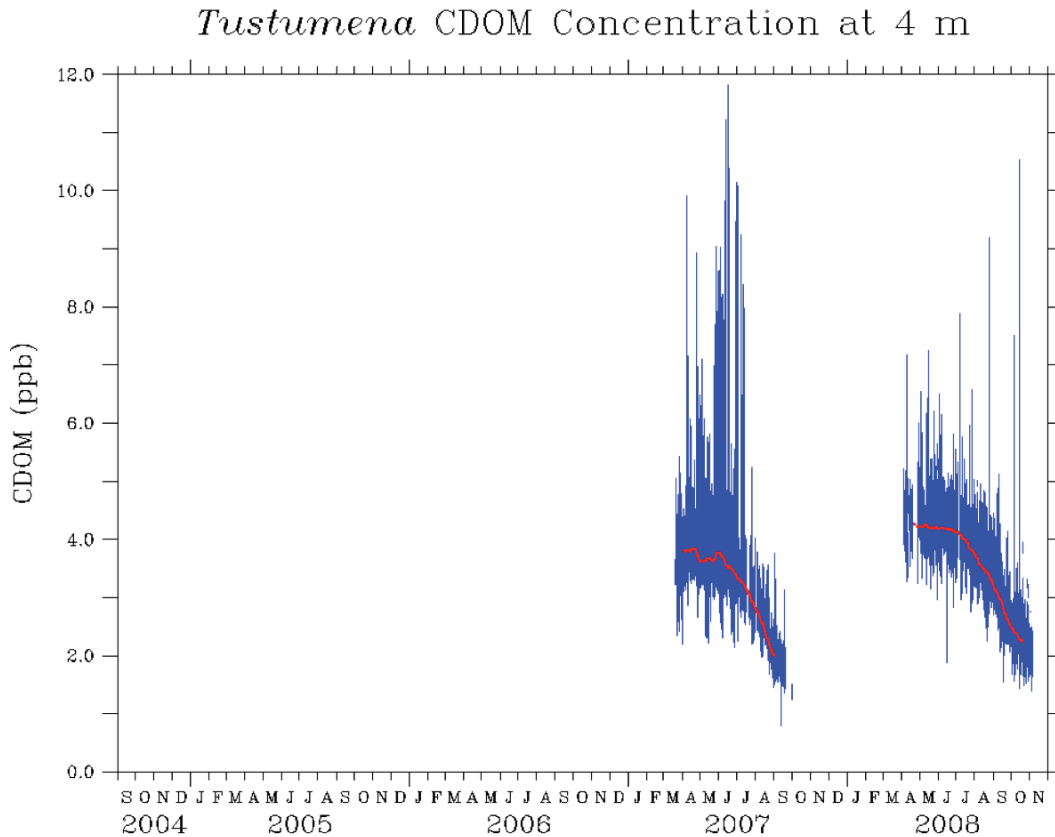


Figure 22. Time series of *Tustumena*'s CDOM concentration at 4 m depth. The smooth red curve represents a 30-day running mean of the observations.

The CDOM concentration is expressed in units of quinine dihydrate equivalent concentration in parts per billion. CDOM is derived from the breakdown of terrestrial humic substances (Kirk, J. T. O., 1983) which are usually delivered to the sea via rivers and streams; therefore the CDOM concentration is thought to be a tracer of terrestrial runoff. Figure 22 shows portions of two annual cycles of CDOM in the study region. CDOM was relatively high in the spring and decreased over the summer and autumn, probably due to photobleaching (Vodacek, A., Blough, N., DeGrandpre, M., Peltzer, E., and Nelson, R., 1997) and dilution by low-CDOM melt water runoff. Generally the CDOM concentration was fairly homogenous along the ferry route; therefore it did not reveal much information about the influence of terrestrial runoff. The map in Figure 23 shows the largest observed horizontal CDOM gradient, which occurred in July 2008.

CDOM was about 4 ppb between Homer and the north end of Kodiak Island, and increased to 7.8 ppb in narrow Kuprenhof Strait near Kodiak and Port Lions.

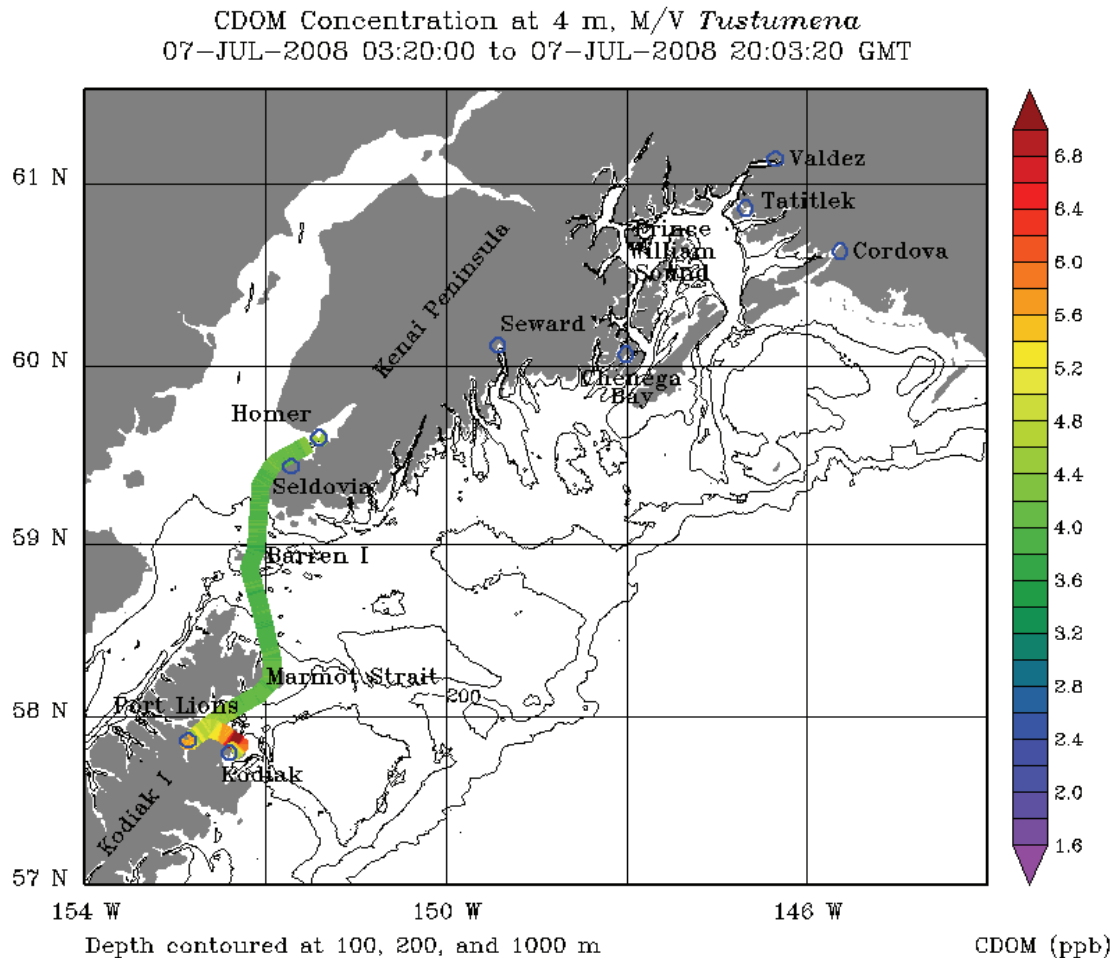


Figure 23. The CDOM concentration along *Tustumena*'s track on 7 July 2008 shows the highest values near Kodiak.

The transmittance of a beam of light through water is a measure of the relative sediment concentration. Less light is transmitted with increasing sediment. As mentioned in the Methods section, owing to fouling it was not possible to compute the attenuation coefficient directly, but we did compute  $c - c_{fw}$ , the difference in attenuation coefficients between seawater and the ship's drinking water. Figure 24 illustrates the time series of  $c - c_{fw}$  during the *Tustumena*'s deployment period. The attenuation coefficient difference lies between  $-1.3$  and  $17 \text{ m}^{-1}$ . For reference, the attenuation coefficient of pure water at 660 nm is approximately  $0.4 \text{ m}^{-1}$  (Morel, A., 1974), but the fresh water in the ship's drinking water tanks was not pure. Instances when  $c - c_{fw}$  was negative imply that the oceanic water was clearer than the ship's fresh water. The map in Figure 25 shows how

the attenuation coefficient varied along the ship's track on 12-14 July 2005, the same time period as covered in Figure 12 for temperature and Figure 14 for salinity. High attenuation, implying high sediment concentration, was observed in Resurrection Bay near Seward, and that corresponded to fresher, warmer water in the bay. This was likely

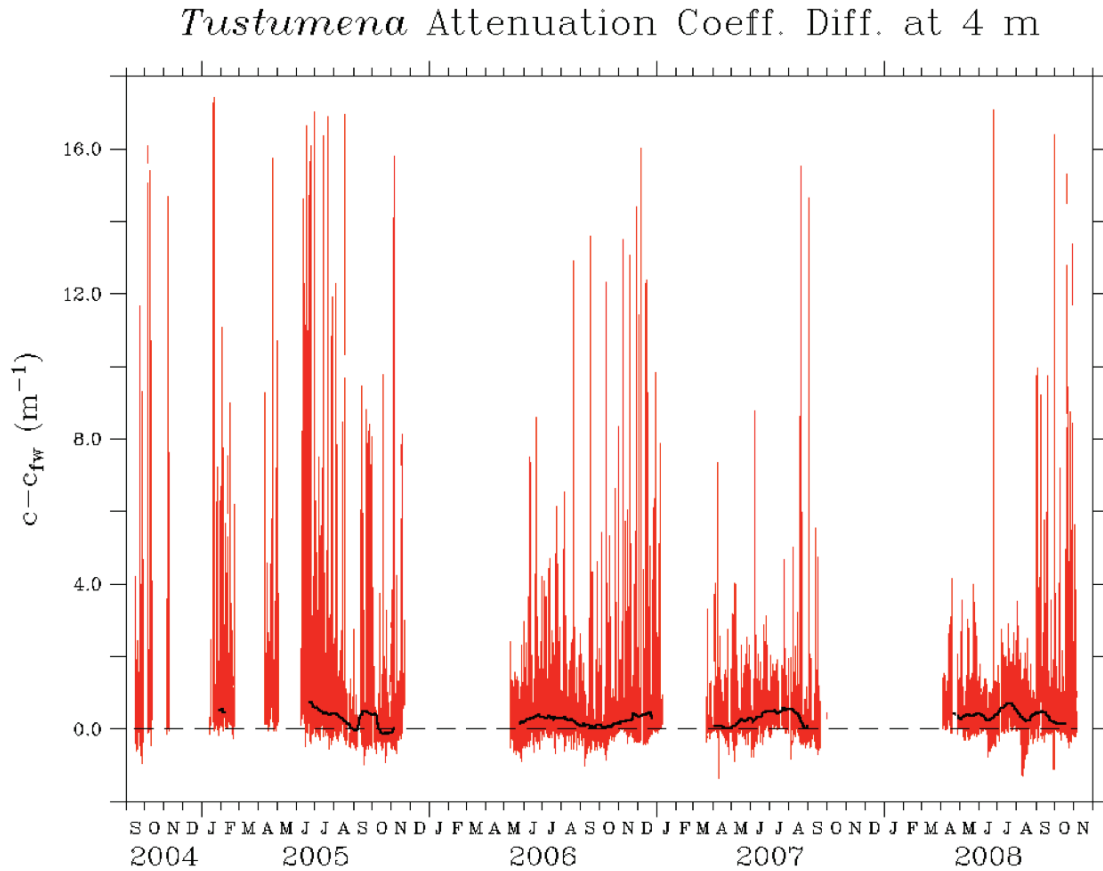


Figure 24. Time series of *Tustumena*'s attenuation coefficient difference,  $c - c_{fw}$ , between seawater at 4 m depth and fresh water. The smooth black curve represents a 30-day running mean of the observations.

due to glacial melt water that formed a low-salinity surface layer that was heated by the sun. Notice also the relatively clearer, colder and saltier water in the Barren Islands, caused by water mixed from below by tidal currents, compared to that on either side.

Attenuation Coefficient Diff.,  $c - c_{tw}$ , at 4 m, M/V *Tustumena*  
 12-JUL-2005 15:39:00 to 14-JUL-2005 23:51:00 GMT

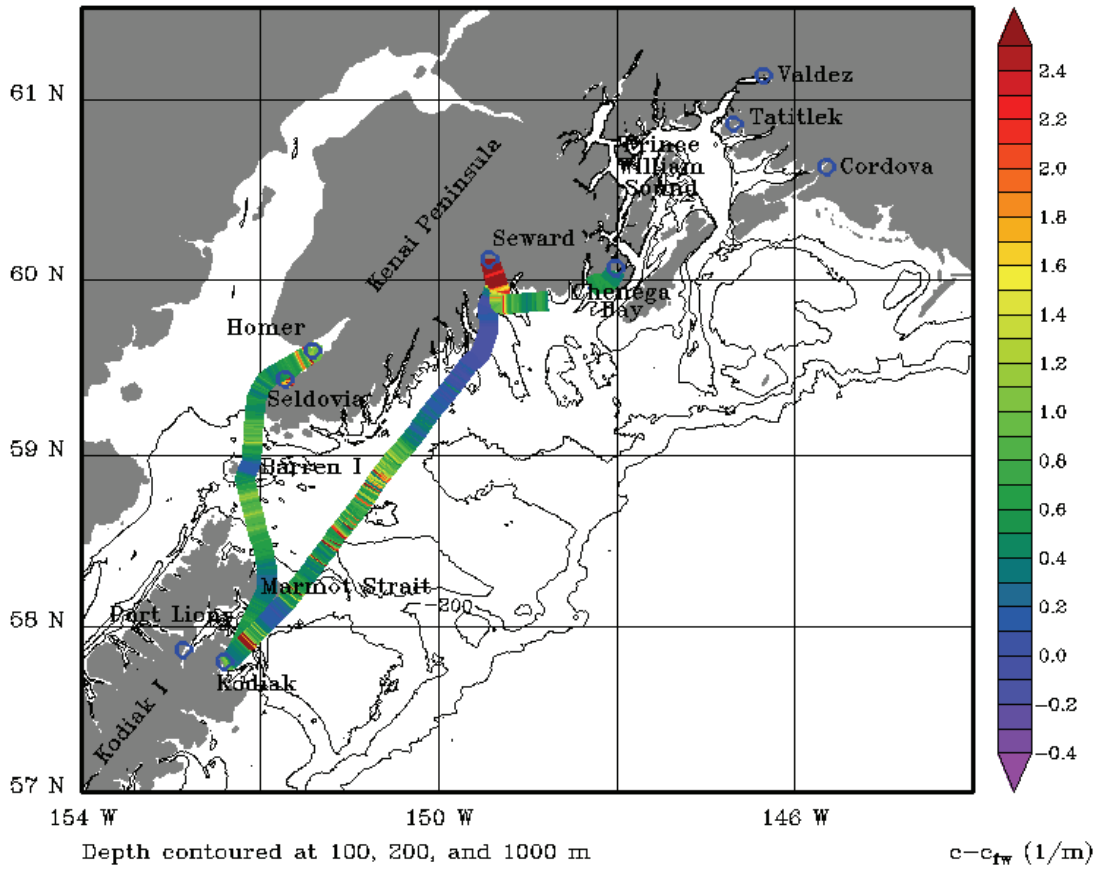


Figure 25. Map of the attenuation coefficient difference along *Tustumena*'s route on 12-14 July 2005.

## Discussion:

We have successfully designed, built, installed and operated for four years an underway oceanographic observing system on the Alaskan ferry *Tustumena*. During that time we made over 1,500,000 measurements each of temperature, salinity, chlorophyll, CDOM and optical attenuation and over 54,000 measurements of nitrate while the ferry traced and retraced over 300,000 km of ocean. These measurements characterize the large regional and temporal variability along the ship's track. The maps (Figures 12, 14, 17, 19, 23 and 25) give snapshots of the spatial variability, and complete map-based movies are available on the project's web site at [http://www.pmel.noaa.gov/foci/GEM/alaska\\_ferry/GEM\\_data.html](http://www.pmel.noaa.gov/foci/GEM/alaska_ferry/GEM_data.html). By viewing them simultaneously one can get a feel for where, when and how the various environmental parameters interact.

The time series plots (Figures 11, 13, 18, 20 and 24) mix the spatial and temporal dependence together. That makes it difficult to discern regional differences and the temporal evolution at a single location. Therefore it is instructive to isolate the temporal signals and form climatological averages and anomalies. Data were extracted at the following discrete points: Kachemak Bay near Homer, Kennedy Entrance between Seldovia and the Barren Islands, the narrow channel within the Barren Islands, and Marmot Strait. Kachemak Bay was chosen as a harbor with glacial runoff at its head. Kennedy Entrance is one of the two main, deep entrances through which the Alaska Coastal Current enters Shelikof Strait on the west side of Kodiak Island. The narrow channel within the Barren Islands and Marmot Strait, between Marmot and Afognak Islands, have strong tidal mixing. We extracted the oceanographic measurements within square boxes, 1-2 km on a side (5-10 km for less-frequently sampled nitrate), centered on each site. For each site this produced a time series with mostly missing values interspersed with short bursts of actual measurements as the ship passed through the box. The short bursts were not independent of each other, which must be taken into account. At 13 kt or 6.8 m/s, the ship traveled 1 km in 2.5 minutes. Thus each box was crossed in less than an hour, and no box was re-entered within that hour. The data were averaged into hour-long increments giving one independent estimate for each box crossing. Figure 26 shows the hourly temperature measurements as black X's. These data were averaged into monthly values centered at mid-month. Each January, etc., was averaged together to form an annual climatological time series and plotted over 4 cycles as shown by the green curves. The red and blue panels represent the monthly positive and negative anomalies about the annual climatological values. Owing to the fact that the ferry and/or the instruments did not run through all seasons of all years, caution is required in interpreting the results. The summer climatology maximum is well defined, being measured in all 4 years, but the late-autumn/early-winter climatology is defined by only 1 or 2 years of observations.

From Figure 26, largest temperature range is in semi-enclosed Kachemak Bay, the next in open Kennedy Entrance and the least in the tidally mixed Barren Islands and Marmot Strait. Also shown are the results for the entire Kodiak-Homer route (within a 222 km N-S x 74 km E-W box) and for the GAK1 CTD time series maintained by the University of

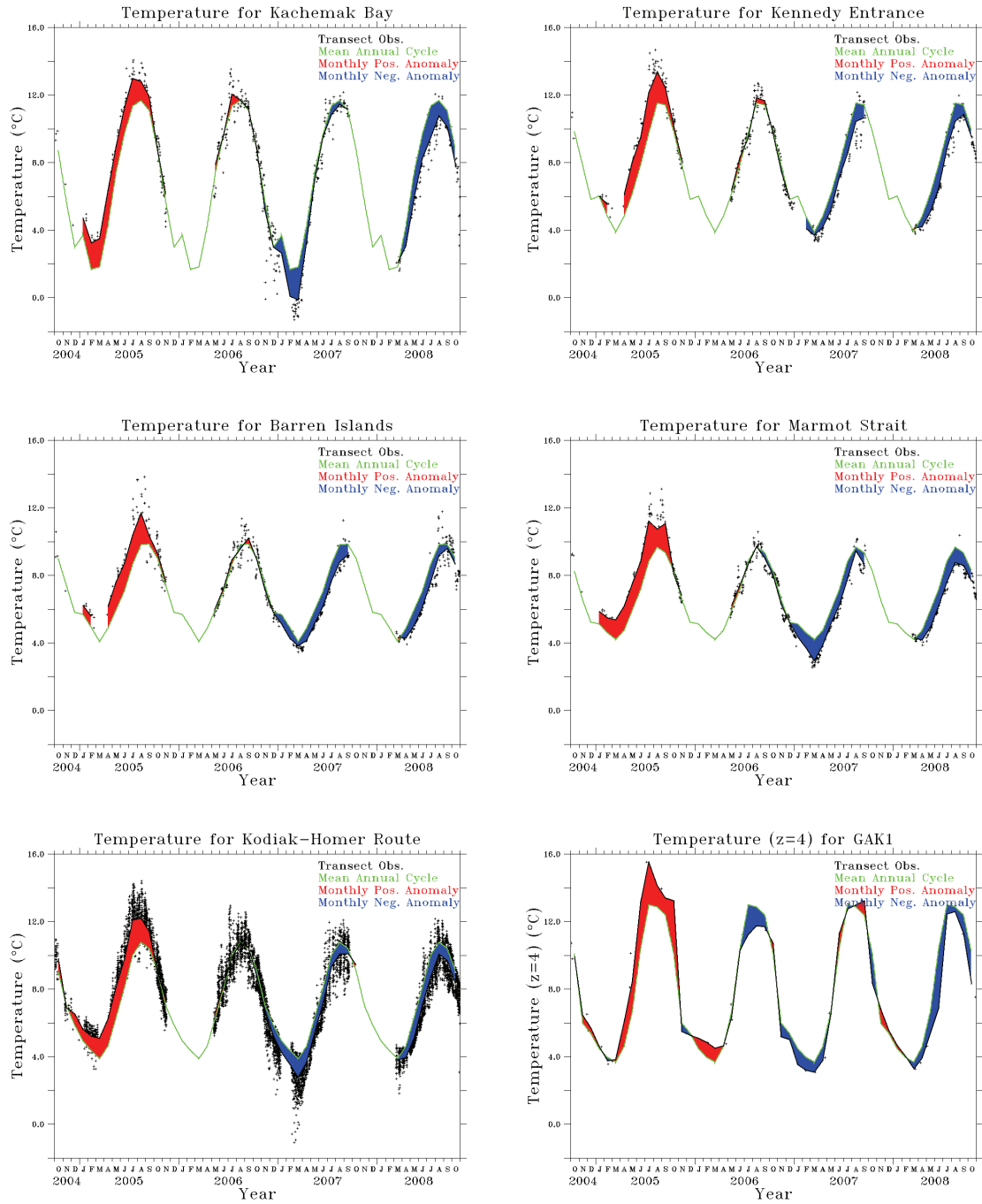


Figure 26. The temperature climatology centered on Kachemak Bay, Kennedy Entrance, the Barren Islands and Marmot Strait. The black X's represent the average value for each time the ship crossed a box. The green curve is the monthly averaged annual cycle, and the red and blue panels represent monthly positive and negative anomalies about the average annual cycle. Also shown are hourly values for a large box encompassing the entire Kodiak-Homer route. For GAK1, the X's represent monthly averages from CTD observations interpolated to 4 m.

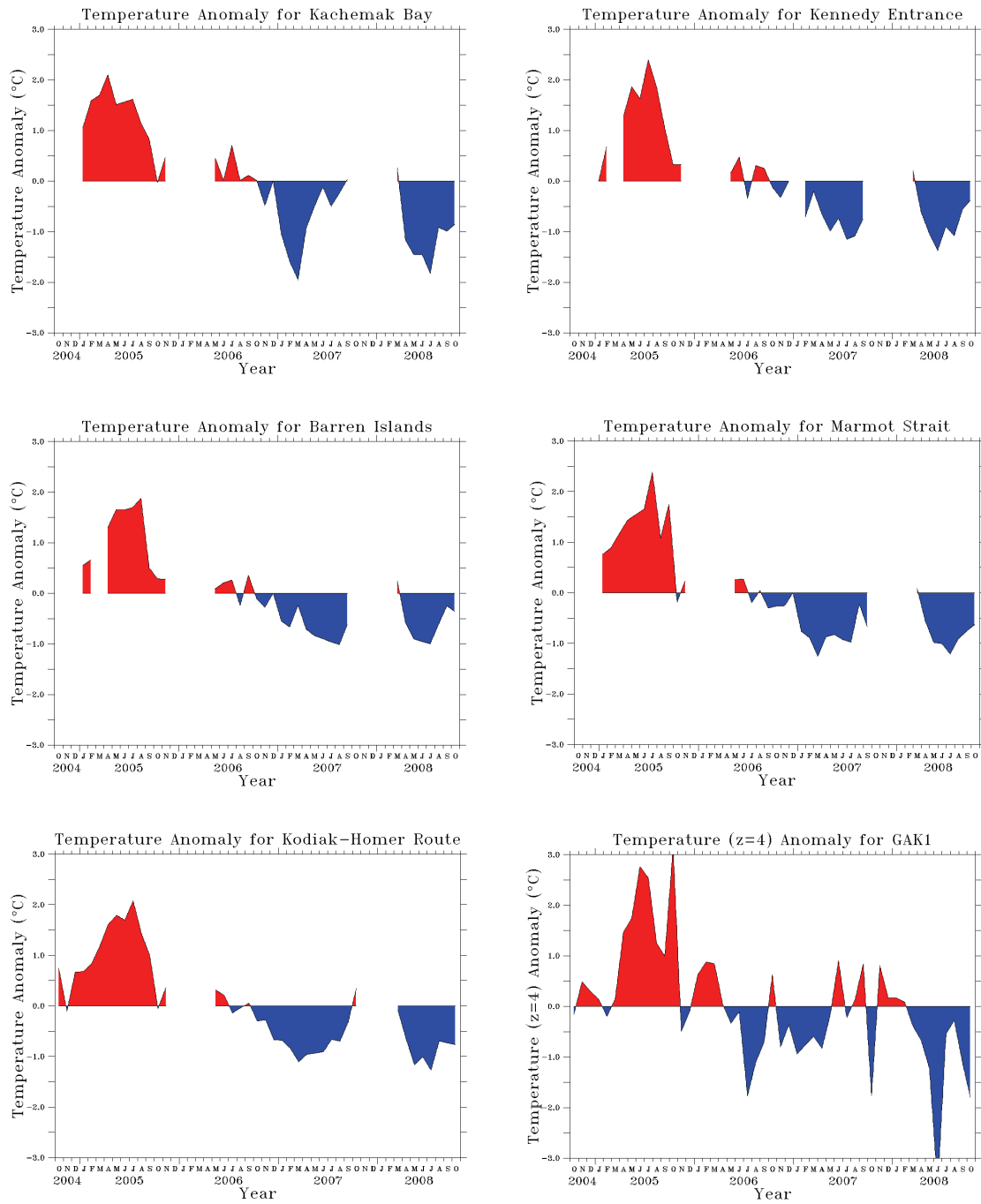


Figure 27. The temperature anomaly for Kachemak Bay, Kennedy Entrance, the Barren Islands, Marmot Strait, the Kodiak-Homer route and GAK1. The red and blue panels represent monthly positive and negative anomalies about the average annual cycle.

Alaska (Weingartner, T., Danielson, S. L., and Leech, D., 2010). The amalgamated Kodiak-Homer time series has the advantage of many more data points than that for any fixed location because the ferry spent most of its time on this route. Figure 27 shows the temperature anomaly time series extracted from Figure 26. Most striking is the fact that the temperature anomalies are very similar at the six sites, even though the individual time series are rather different (Figure 26). Evidently the climatological temperature anomaly is region-wide.

The salinity climatologies and anomalies are shown in Figures 28 and 29. The salinities between the four *Tustumena* sites differ more than the temperatures (Figure 26) with Kachemak Bay showing the greatest range owing to the influence of local runoff. The curves in the tidally mixed Barren Islands and Marmot Strait are much flatter, as is that for the entire Kodiak-Homer route because the ferry spends most of its transit time in deep water, away from ports influenced by local runoff. The salinity anomalies are similar amongst all the sites, but with GAK1 showing the greatest amplitude.

River discharge into the Gulf of Alaska stems from melting snow and ice (Royer, T. C., 1982); therefore a warmer climate should accompany more discharge and a fresher ocean and vice versa. The temperature (Figure 27) and salinity (Figure 29) anomalies bear this out. A warm, fresh regime from autumn 2004 through mid-winter 2006 switched to a generally cool, salty period through October 2008. The near-surface *Tustumena* measurements prove that oceanographic anomalies observed at GAK1 extend to the larger Alaska Coastal Current system. Research at GAK1 shows that the anomalies are correlated with depth (Royer, T. C., 2005; Royer, T. C. and Grosch, C. E., 2006; Sarkar, N., Royer, T. C., and Grosch, C. E., 2005; Weingartner, T. J., Danielson, S. L., and Royer, T. C., 2005). Thus the ocean warms and freshens, or cools and becomes saltier in concert, over the entire water column on the continental shelf.

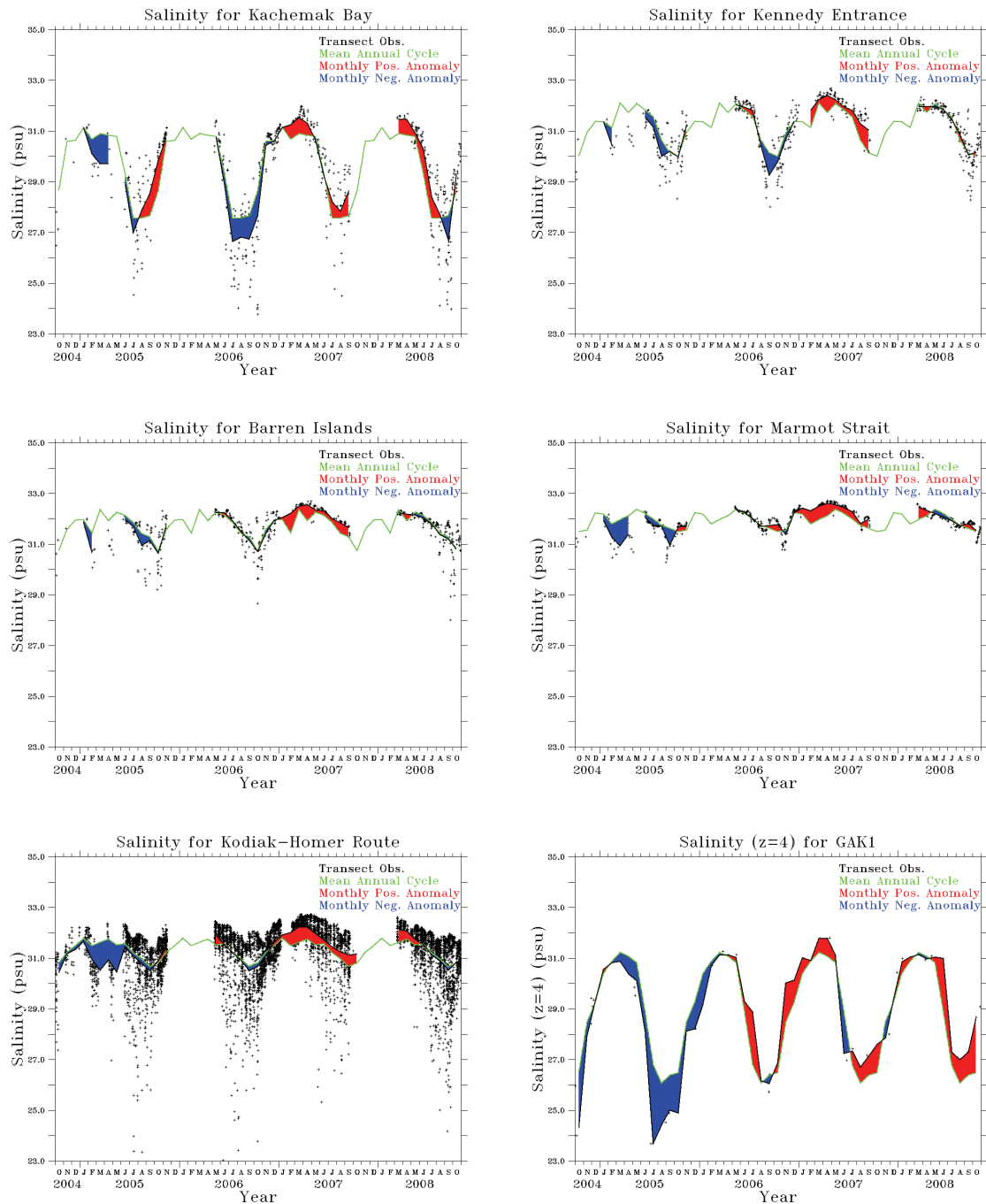


Figure 28. The salinity climatology centered on Kachemak Bay, Kennedy Entrance, the Barren Islands and Marmot Strait. The black X's represent the average value for each time the ship crossed a box. The green curve is the monthly averaged annual cycle, and the red and blue panels represent monthly positive and negative anomalies about the average annual cycle. Also shown are hourly values for a large box encompassing the entire Kodiak-Homer route. For GAK1, the X's represent monthly averages from CTD observations interpolated to 4 m.

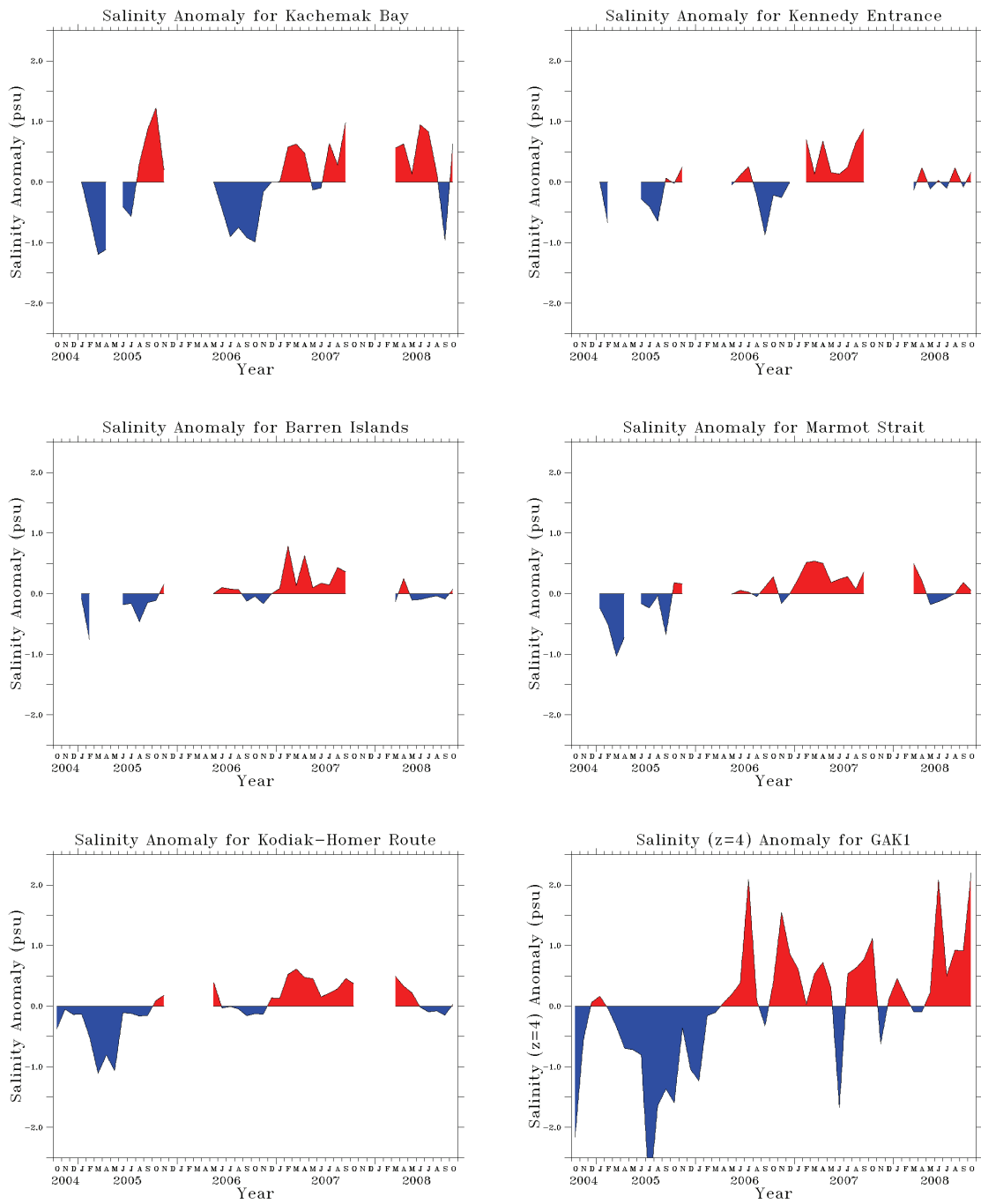


Figure 29. The salinity anomaly for Kachemak Bay, Kennedy Entrance, the Barren Islands, Marmot Strait, the Kodiak-Homer route and GAK1. The red and blue panels represent monthly positive and negative anomalies about the average annual cycle.

The Pacific Decadal Oscillation (PDO) is an index of basin-wide sea surface temperature fluctuations in the Pacific Ocean (Ebbesmeyer, C. C., Cayan, D. R., Milan, D. R., Nichols, F. H., Peterson, D. H., and Redmond, K. T., 1991; Mantua, N., Hare, S., Zhang, Y., Wallace, J., and Francis, R., 1997; Zhang, Y., Wallace, J., and Battisti, D., 1997). Figure 30 illustrates the PDO time series for the period of the *Tustumena* observations (Mantua, N. J., 2010). The PDO transitioned from warm to cool conditions similar to the *Tustumena* temperature anomalies of Figure 26, indicating that the ferry measurements have detected this climate signal.

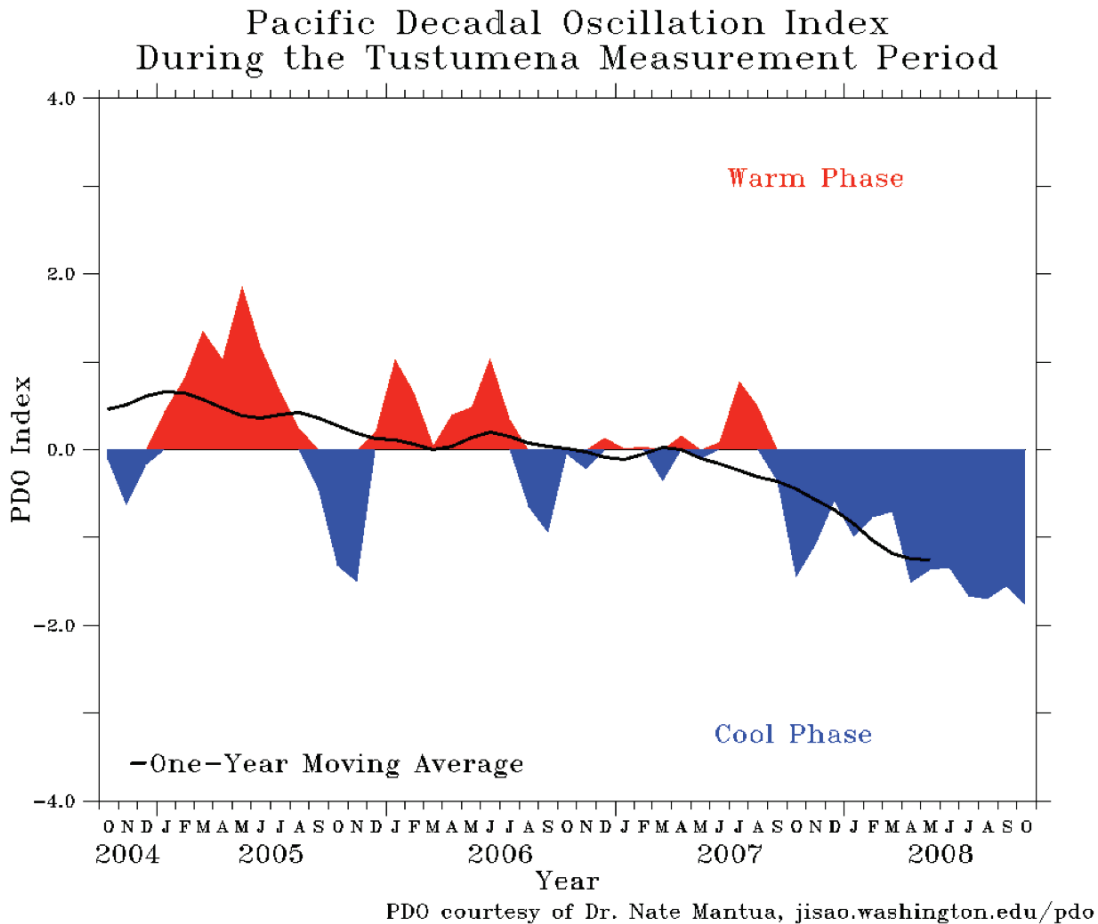


Figure 30. The Pacific Decadal Oscillation (PDO) index during the *Tustumena* measurement period.

*Tustumena* measured the dissolved nitrate and chlorophyll concentrations – two biophysical parameters relating to the ecosystem. Figures 31-34 show the climatology and anomaly time series – the longest such available in the Gulf of Alaska. Nitrate and chlorophyll have a smaller annual amplitude in the two strongly mixed regions – the Barren Islands and Marmot Strait. The anomalies are less similar across the region than for temperature and salinity, but there is evidence for positive anomalies at the beginning and end of the record and negative anomalies in the middle. This implies that the greater

availability of nitrate leads to a greater phytoplankton standing stock, the same conclusion drawn from the carbon-nitrate plot of Figure 21. Nitrate and chlorophyll observations are not available at GAK1; thus no comparisons are possible there.

As the maps in Figures 23 and 25 show, the CDOM concentration and the attenuation coefficients have very local peaks, usually due to nearby river inputs of terrestrial material that soon settles out. Compared to temperature and salinity, their anomalies (not plotted here) have higher frequency and are less similar across the region.

This project has been very successful. The Volunteer Observing Ship measurements were made with no cost for ship time. We recommend that the observations be reinstated on *Tustumena* and added to other Alaskan ferries in Prince William Sound and southeast Alaska. Dissolved oxygen sensors should be added to the instrument suite to detect phytoplankton blooms that have sunk toward the pycnocline, but still saturate the upper water column with oxygen. Discrete samples of salinity, nitrate, chlorophyll and oxygen are necessary for instrument calibration. With three ships, a full-time person is required to oversee the daily observations downloaded via satellite, check for instrument problems and update a web site with data and graphics. One staff person should ride each ferry at least monthly on calibration trips chosen on routes and at times for which the observations achieve their maximum dynamic range. It is absolutely critical that local personnel be made available for a few hours each week to clean the instruments and provide simple maintenance in one port-of-call on each route.

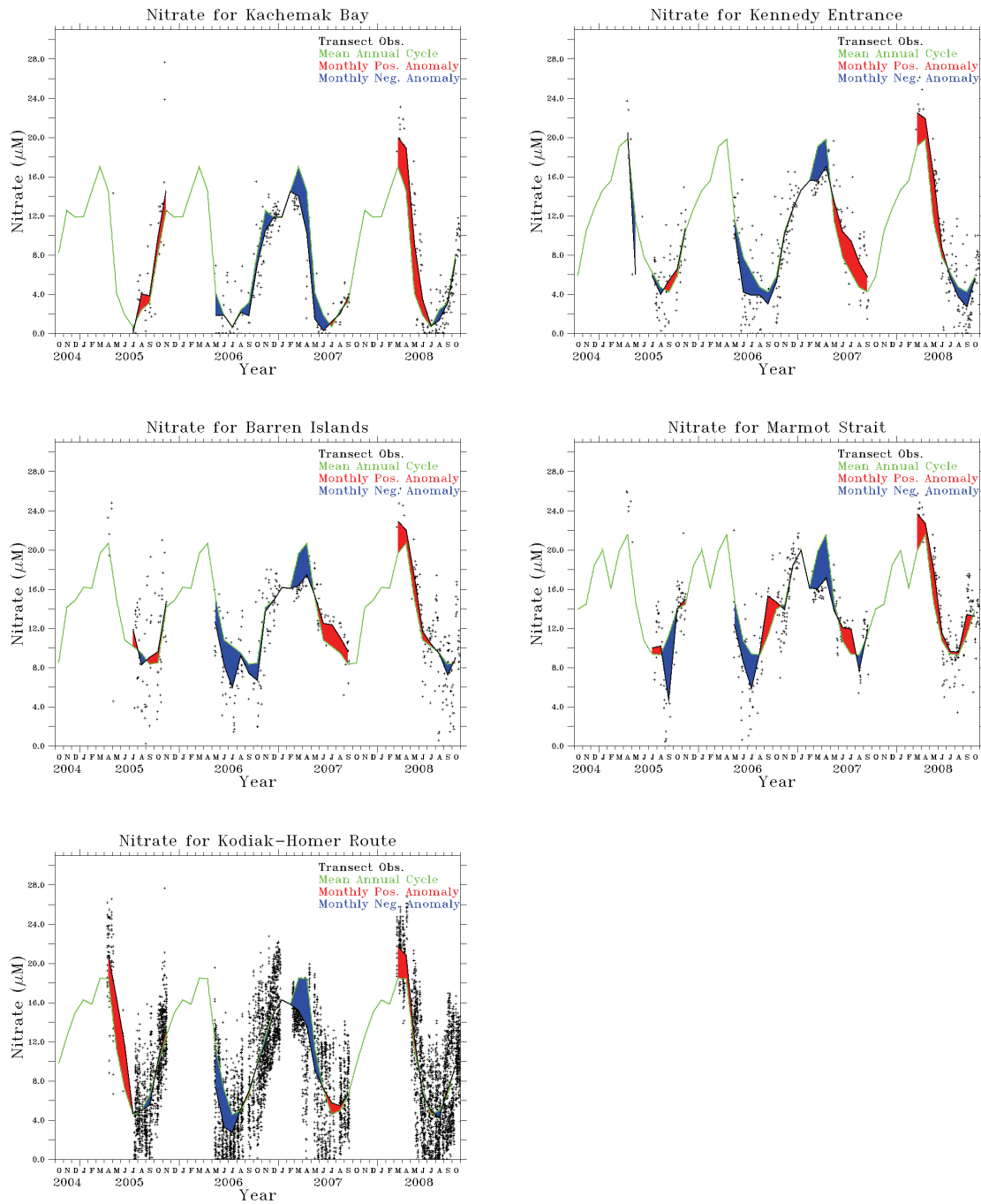


Figure 31. The nitrate climatology for Kachemak Bay, Kennedy Entrance, the Barren Islands and Marmot Strait. The black X's represent the average value for each time the ship crossed a box. The green curve is the monthly averaged annual cycle, and the red and blue panels represent monthly positive and negative anomalies about the average annual cycle. Also shown are hourly values for a large box encompassing the entire Kodiak-Homer route.

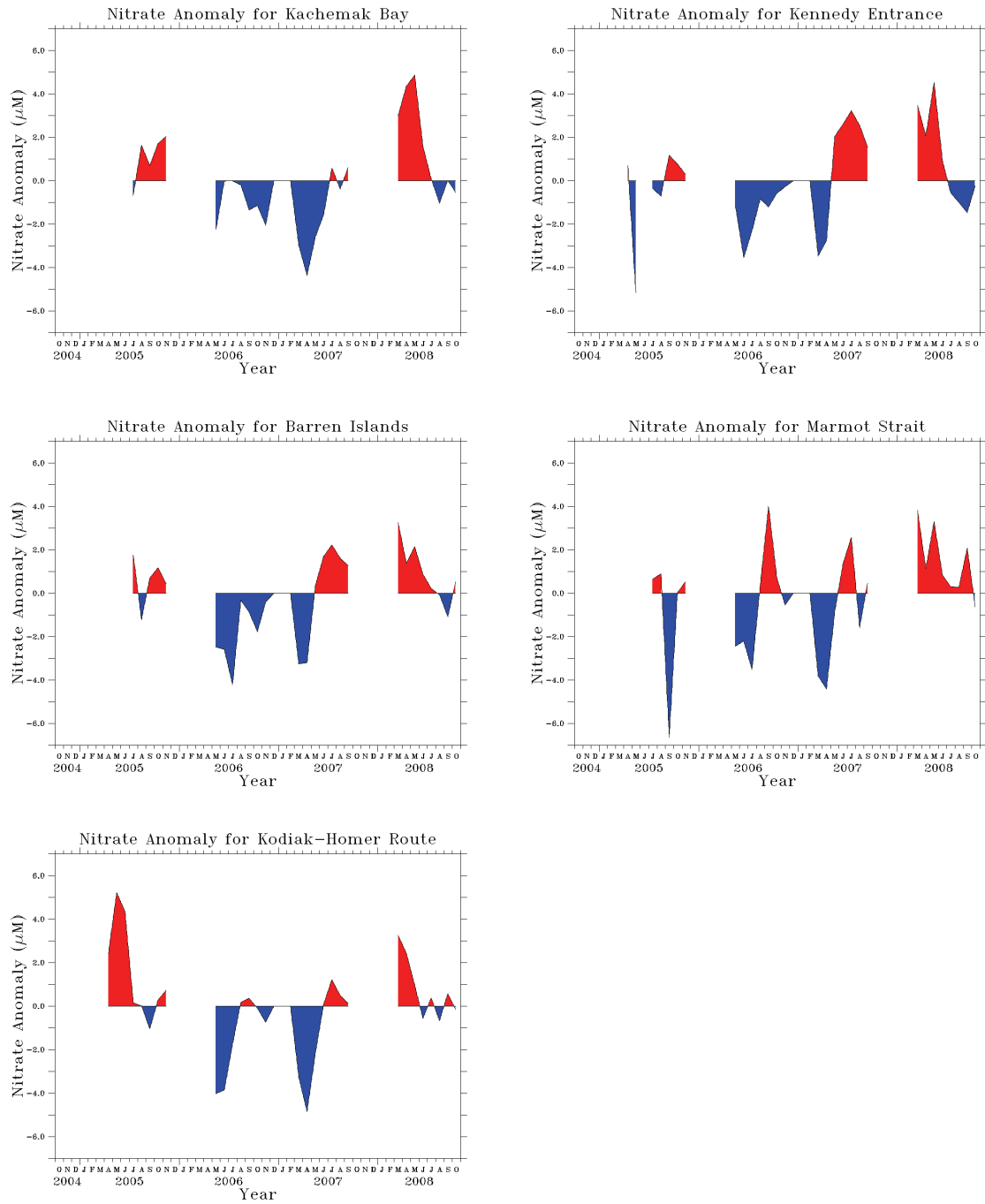


Figure 32. The nitrate anomaly for Kachemak Bay, Kennedy Entrance, the Barren Islands, Marmot Strait and the Kodiak-Homer route. The red and blue panels represent monthly positive and negative anomalies about the average annual cycle.

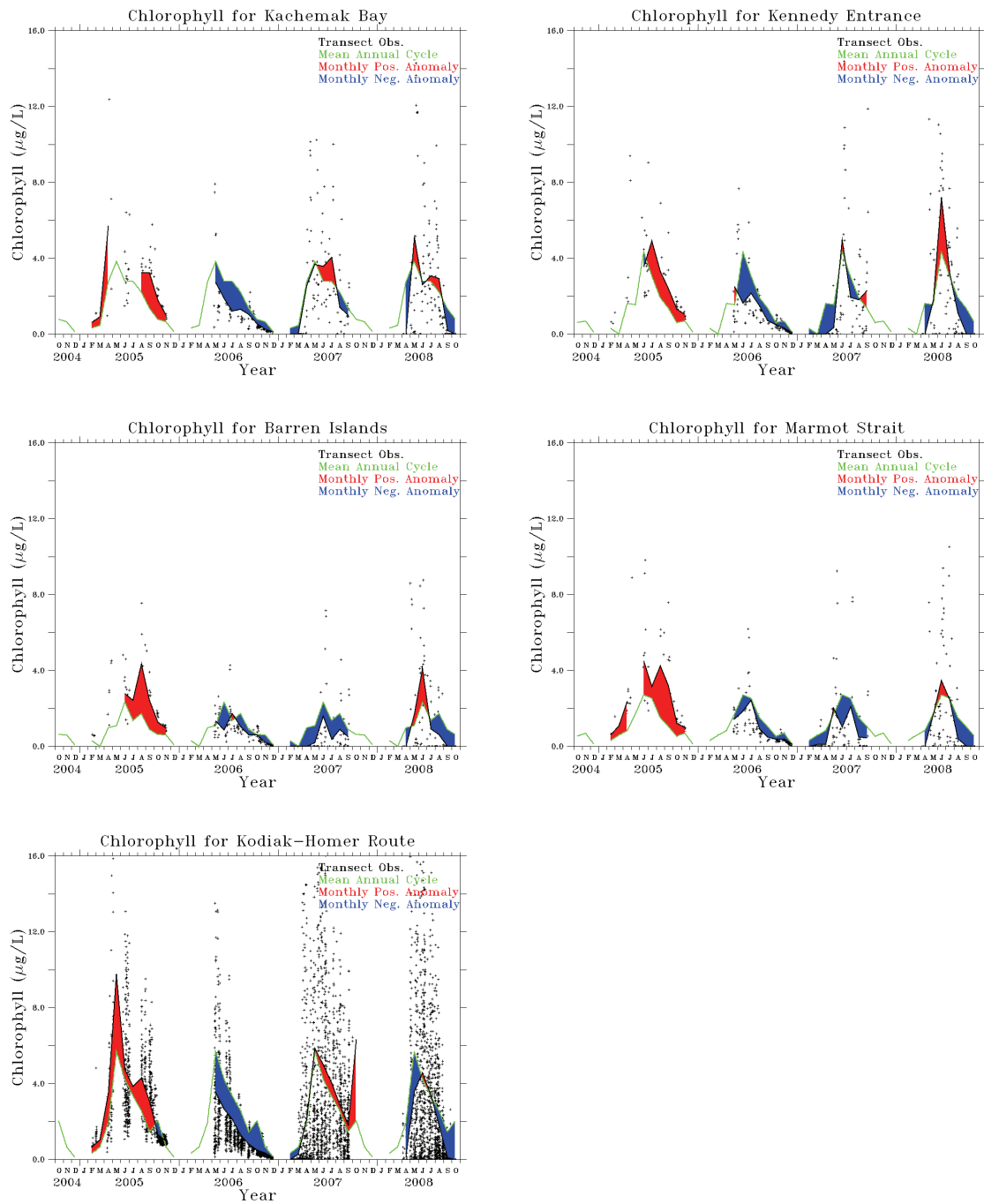


Figure 33. The chlorophyll climatology for Kachemak Bay, Kennedy Entrance, the Barren Islands and Marmot Strait. The black X's represent the average value for each time the ship crossed a box. The green curve is the monthly averaged annual cycle, and the red and blue panels represent monthly positive and negative anomalies about the average annual cycle. Also shown are hourly values for a large box encompassing the entire Kodiak-Homer route.

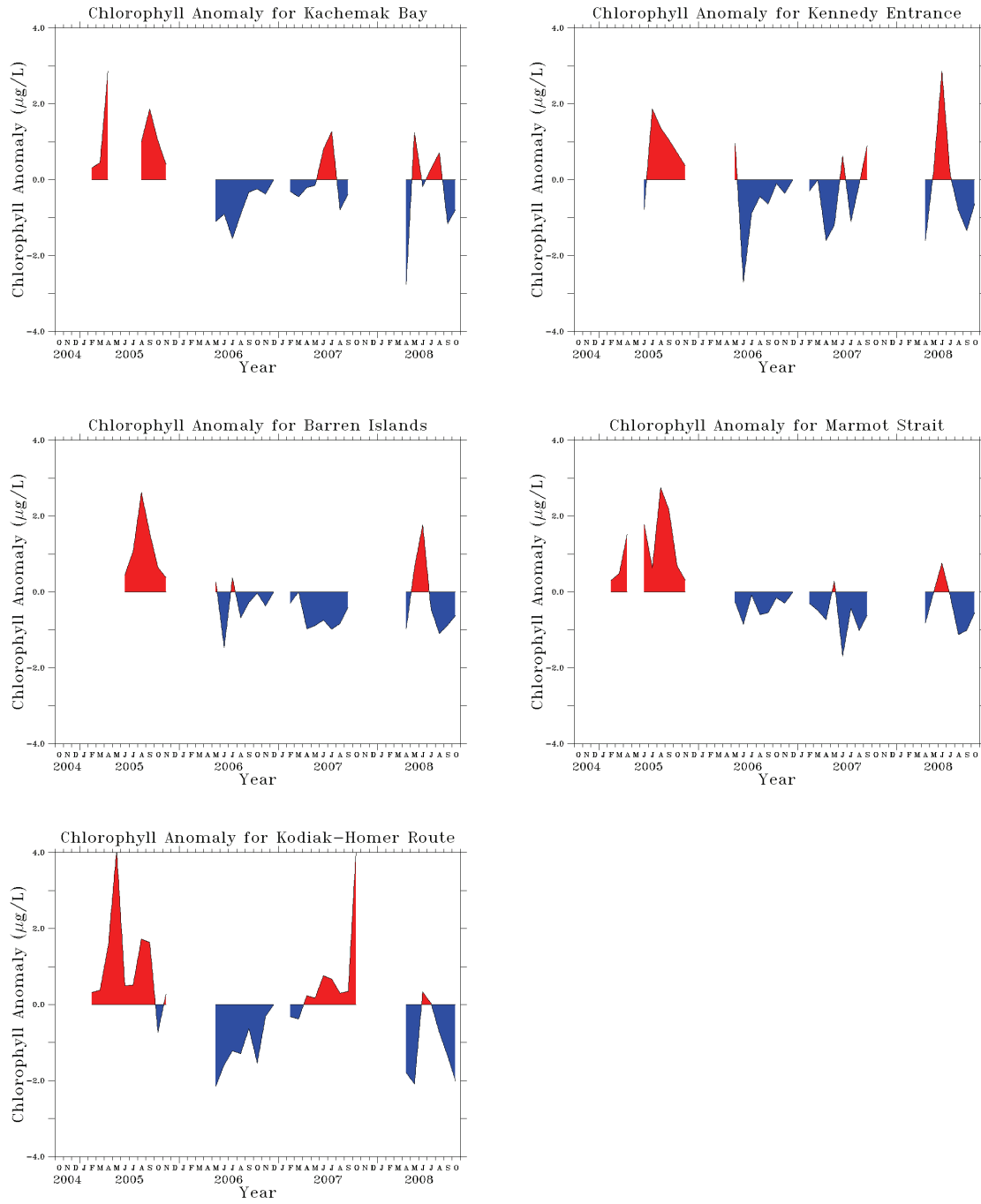


Figure 34. The chlorophyll anomaly for Kachemak Bay, Kennedy Entrance, the Barren Islands, Marmot Strait and the Kodiak-Homer route. The red and blue panels represent monthly positive and negative anomalies about the average annual cycle.

## **Conclusions:**

We successfully designed, built, installed and operated an underway-oceanographic observing system on the Alaskan ferry *Tustumena*. The system had the following novel features:

1. Hourly data transmittal to PMEL via Iridium satellite,
2. Two-way Iridium satellite communication between the data acquisition system and PMEL,
3. Leak detection with automatic seawater supply cut off,
4. Freshwater backflushing upon arrival in ports to reduce the time between manual cleanings,
5. Automatic cessation of measurements while in ports to conserve data transmission and storage,
6. Automatic e-mail notification of system problems,
7. A passenger display terminal showing the ferry position and the latest oceanographic measurements, and
8. Successful application of an optical sensor to measure dissolved nitrate concentrations on an underway system.

We measured a four-year time series of near-surface oceanographic properties over a 1000 km of ferry route in the Gulf of Alaska. The longevity of the measurements was sufficient that multiyear monthly means and their anomalies have been calculated, and climatic signals emerge. Similarity to the temperature and salinity anomalies at GAK1 prove that long-term climate measurements there apply to a wider region of the Gulf of Alaska. Temperature and salinity anomalies in the Alaska Coastal Current transitioned from relatively warm, fresh ocean conditions to cool, salty ones during the *Tustumena* measurement period. New nitrate and chlorophyll anomalies indicate that relatively higher nutrients coincide with a greater phytoplankton stock and vice versa.

## **Outreach:**

Web Page Development: The project web page ([http://www.pmel.noaa.gov/foci/GEM/alaska\\_ferry](http://www.pmel.noaa.gov/foci/GEM/alaska_ferry)) provides

1. An introduction,
2. Technical details,
3. Data plots, movies and data downloads, and
4. Program information.

Exhibits: An electronic display in the ship's passenger lounge gave a changing slide show of

1. Sea surface temperature along the ship track, updated every few minutes,
2. Educational information about the oceanic observations, and
3. Google Earth virtual fly-overs showing the ferry's location and the surrounding geography.

Conference Presentations: See **Other References**.

**Acknowledgments:** We acknowledge and thank the following individuals and organizations: The *Exxon Valdez* Trustee Council for funding; Phil Mundy who as the EVOS Trustee Council Science Director initiated the GEM program and supported ferry monitoring; the Alaska Marine Highway System for allowing us to instrument *Tustumena* with special thanks to Port Engineer Paul Johnsen, Chief Port Engineer George Poor, Captains J. P. Stormont and Robert Crowley, Chief Engineer Ken Hammer, General Manager George Capaci, and the crew of *Tustumena*; naval architect Andrew K. Bennett and marine engineer Chris P. Staehli of Art Anderson Associates, Seattle, for design assistance and verification; Seward Ships Drydock for wiring and plumbing *Tustumena*; Steve Baird and other KBRR staff members who faithfully cleaned and maintained the instruments approximately weekly when the ship docked at Homer; Eric Wisegarver and Peter Proctor of PMEL who rode the ship, collected calibration samples and analyzed the nitrate samples; Peggy Sullivan of PMEL who designed and ran the web site; Oriana Badajos who analyzed the chlorophyll samples; the ferret group at PMEL who built a wonderful data analysis tool; Peter Hagen who served as liaison between the Trustee Council and NOAA researchers and provided valuable administrative guidance; Tom Royer of Old Dominion University who began the GAK1 observational program and supports oceanographic monitoring in the Gulf of Alaska.

**Appendix:** Details of the Underway Seawater Monitoring System Control. The underway sampling system was designed and built by Antonio J. Jenkins to control the instruments, clean them by backflushing with fresh water, sample them and transmit the data to PMEL via Iridium satellite. A LabVIEW program running on a Linux computer controlled the primary functions. The system had four modes of operations as follows:

1. Sleep Mode - The system was normally in Sleep Mode while in port. While asleep it could:
  - a. Read global positioning system (GPS) input to determine if the ship was moving and, if so, enter Normal Mode, or
  - b. Respond to a local user via keyboard entries in the main instrument box and enter Clean, Calibrate or Normal Mode.
2. Clean Mode – This mode was intended for use during cleaning or testing of the system. In this mode the Local User was shown a test panel screen where all system controls were available, and all instrument inputs could be viewed and tested. While in Clean Mode, the user typically controlled the pump and backflush valves while viewing the outputs of all instruments.
3. Calibrate Mode – This mode was intended for use while running deionized (DI) water through the system during calibration. DI water was delivered by closing the manual saltwater valve, opening the manual sample valve and providing DI water at modest pressure (2 to 3 psi) and moderate flow (1 to 2 gpm) as an input to the sample valve. This mode loaded the Initialization File as per Normal Mode (see below), but logged data at 5-second intervals, ignoring the low-flow indicators as described below. It presented the user with start and stop buttons to allow time to setup the DI flow before logging started.
4. Normal Mode – Normal mode was used most often. The system prompted the Local User to select the Initialization Screen for user input. If there was no response after 30 seconds on the keyboard within the main system box, the system skipped the Initialization Screen and began sampling, logging, and transmitting data and error messages (if necessary) to PMEL and enabled Remote User features. If selected, the Initialization Screen had a graphical user interface to allow the configuration of all programmable settings through the Initialization File that specified the following:
  - A) Com ports for various instruments
  - B) Analog input channel names, voltage ranges, number of samples to average per recorded value, and the time between each sample (not between time averages)
  - C) Initialization of three file types: INST, ISUS and NAS files. The INST files held recorded digital data from the remote temperature sensor, thermosalinograph (TSG), GPS, and all analog input channels. The ISUS files held data from the Satlantic in situ ultraviolet spectrophotometer (ISUS) nitrate sensor. The NAS files held data from the EnviroTech Nutrient Analyzing System (NAS, installed for part of the 2005 field season).
  - D) Time increment between each set of averaged values appearing in the INST files
  - E) Instruments to be logged by the INST files

- F) Writing some ISUS data to INST files and/or some INST data to ISUS files
- G) Time between each wake-up of the ISUS. All ISUS data were logged from 45 seconds before ISUS wake-up to 45 seconds after the last ISUS data character was received.
- H) Rate (hourly or daily) at which data were transmitted to PMEL via the Iridium satellite link
- D) User-configurable criteria for water flow-rate quality
  - a) Set the pressure-difference threshold over a prescribed averaging time interval (pressure measured approx. once per second) to initiate a system reaction. A large difference as measured by a pair of pressure sensors could indicate clogging. The system was set to react if the one-minute-average exceeded 1.5 volts corresponding to a pressure difference of approx. 15 psi across the strainer.
  - b) Set the flow-rate threshold over a prescribed averaging time interval (flow measured approx. once per second) to initiate a system reaction. Slow flow could indicate clogging. The system was set to react if the one-minute-averaged flow decreased below 3 Hz (approx. 0.2 gpm).
  - c) If either or both thresholds (a) and (b) were met the system reacted as follows:
    - i) Stop the pump, wait 1 minute and restart the pump.
    - ii) Cycle power to the pump 3 times if (i) failed to rectify the problem.
    - iii) Backflush the strainer with fresh water for 10 minutes if (ii) failed.
    - iv) Repeat steps (i)-(iii) until a prescribed number of backflushes (usually 2) were attempted within a prescribed time period (usually 30 minutes).
    - v) If (iv) failed to move the pressure difference and flow rate beyond their error thresholds, the system stopped logging data, conducted a final backflush to fill the lines with freshwater, shut-off the pump, sent an Iridium message alert to PMEL, and entered Sleep Mode.
- J) Drip sensor sensitivity threshold. An electrical sensor in the bottom of the main instrument box could detect water that leaked there. If drip sensor values exceeded the threshold, the pump would stop, seawater flow would stop, freshwater flow would be blocked, the system would send an Iridium message to PMEL describing the leak condition, and the system would enter the “stop gracefully and wait” state.
- K) Turn on watchdog updates. The system could be configured to write a timestamp to a watchdog file as often as possible. If running, the watchdog program checked the timestamp for currency, and if not current, the system would restart.
- L) OK button to begin normal operation

Remote User Features: When operating in Normal Mode, a system feature enabled the Remote User to send instructions and files to the system remotely via the Iridium satellite modem. The Remote User options were as follows:

- 1) Send new software to the system to perform a system upgrade. A new LabVIEW executable file could be uploaded to the system's inbox where it was renamed and remained. The main program continued to run until it was sent a command to switch to the new program, or the Local User restarted the software.
- 2) Send a new Initialization File to the system. A new Initialization File could be uploaded to the system's inbox where it was renamed and remained. The main program continued to run using the old Initialization File until sent an appropriate command or the Local User restarted the software. The main program would overwrite the old Initialization File with the new one.
- 3) Send a command to the system as a short character string in a flat ASCII text file. The commands were as follows:
  - a. "Stop gracefully with reboot" – Stop the system gracefully by closing open files and ending all tasks normally, move the old software to a folder named "last known good", move the new software into the starting directory, and reboot the computer. This command was usually given after the Remote User had sent a software upgrade. It was equivalent to Local User pushing the software "Stop" button.
  - b. "Stop immediately with reboot" – Stop the system software immediately and reboot the computer. It was equivalent to the Local User selecting the "File -> Exit" command and then rebooting the computer.
  - c. "Stop gracefully without reboot" – Stop the system gracefully but do not reboot. This command was used to put the system into a stopped state for long periods of time until it could be visited. It was never used remotely because there was no remote way to bring the system back up after this command was executed.
  - d. "Stop immediately without reboot" – Stop the system software immediately but do not reboot the computer. It was equivalent to the Local User selecting the "File -> Exit" command.
  - e. "Stop gracefully and wait" – Stop the system gracefully, but keep the Iridium interface running, awaiting the "start from wait" command.
  - f. "Start from wait" – Check the inbox for a new Initialization File, if found overwrite the existing one, and restart the system with the new file. This command was used in conjunction with the "stop gracefully and wait" command.
  - g. "Stop gracefully then start" – Combines the "stop gracefully and wait" and "start from wait" commands. It was to be used after a new Initialization File was sent to the system remotely.

### **Literature Cited:**

- Armstrong, F. A. J., Stearns, C. R., and Strickland, J. D. H. 1967. The measurement of upwelling and subsequent biological processes by means of the Technicon AutoAnalyzer and associated equipment. *Deep Sea Research* 14: 381-389.
- Booth, B. C., Lewin, J., and Lorenzen, C. J. 1988. Spring and summer growth rates of subarctic Pacific phytoplankton assemblages determined from carbon uptake and cell volumes estimated using epifluorescence microscopy. *Marine Biology* 98: 287-298.
- Cokelet, E. D., Jenkins, A. J., Pegau, W. S., Mordy, C. W., and Sullivan, M. E. 2005. Biophysical observations aboard and Alaskan state ferry. ASLO Summer Meeting: A Pilgrimage Through Global Aquatic Sciences, Santiago de Compostela, Spain, American Society of Limnology and Oceanography, 33.
- Dore, J., Houlihan, T., Hebel, D., Tien, G., Tupas, L., and Karl, D. 1996. Freezing as a method of sample preservation for the analysis of dissolved inorganic nutrients in seawater. *Marine Chemistry* 53: 173-185.
- Ebbesmeyer, C. C., Cayan, D. R., Milan, D. R., Nichols, F. H., Peterson, D. H., and Redmond, K. T. 1991. Seventh Annual Climate (PACLIM) Workshop, Calif. Dep. Water Res. Interagency Ecological Studies Program Tech. Rep. 26, 115-126.
- Frost, B. W. 1993. A modelling study of processes regulating plankton standing stock and production in the open subarctic Pacific Ocean. *Progress In Oceanography* 32: 17-56.
- GHRSSST-PP SST Science Team, 2010. Understanding sea surface temperature. [Available online from <http://www.ghrsst.org/SST-Definitions.html>.]
- Gordon, L., Jennings Jr, J., Ross, A., and Krest, J. 1994. A suggested protocol for continuous automated analysis of seawater nutrients (phosphate, nitrate, nitrite, and silicic acid) in the WOCE Hydrographic Program and the Joint Global Ocean Fluxes Study. WOCE Operations Manual, Vol. 3: The Observational Programme, Section 3.2: WOCE Hydrographic Programme, Part 3.1. 3: WHP Operations and Methods. WHP Office Report WHPO 91-1, WOCE Report.
- Kirk, J. T. O. 1983. Light and photosynthesis in aquatic ecosystems. First ed. Cambridge University Press.
- Lienhard, J. H., IV and Lienhard, J. H., V. 2008. A Heat Transfer Textbook. Third ed. Phlogiston Press, 762 pp.
- Lorenzen, C. 1966. A method for the continuous measurement of in vivo chlorophyll concentration. *Deep Sea Research* 13: 223-227.

- Mantua, N., Hare, S., Zhang, Y., Wallace, J., and Francis, R. 1997. A Pacific interdecadal climate oscillation with impacts on salmon production. *Bulletin of the American Meteorological Society* 78: 1069-1079.
- Mantua, N. J., 2010. The Pacific Decadal Oscillation (PDO). [Available online from [http://jisao.washington.edu/pdo/.](http://jisao.washington.edu/pdo/)]
- Morel, A. 1974. Optical properties of pure water and pure sea water. *Optical aspects of oceanography*, N. Jerlov, Ed., 1-24, Academic Press.
- Powell, C. A., 2010. Cu-Ni alloys – Resistance to corrosion and biofouling. [Available online from [http://www.copper.org/applications/cuni/txt\\_resistance\\_to\\_corrosion.html#physical](http://www.copper.org/applications/cuni/txt_resistance_to_corrosion.html#physical).]
- Redfield, A. C. 1934. On the proportions of organic derivations in sea water and their relation to the composition of plankton. *James Johnstone Memorial Volume*, R. J. Daniel, Ed., 177-192, University Press of Liverpool.
- Royer, T. C. 1982. Coastal freshwater discharge in the northeast Pacific. *Journal of Geophysical Research* 87: 2017-2021.
- Royer, T. C. 2005. Hydrographic responses at a coastal site in the northern Gulf of Alaska to seasonal and interannual forcing. *Deep-Sea Research II* 52: 267-288.
- Royer, T. C. and Grosch, C. E. 2006. Ocean warming and freshening in the northern Gulf of Alaska. *Geophysical Research Letters* 33: 1-6.
- Sarkar, N., Royer, T. C., and Grosch, C. E. 2005. Hydrographic and mixed layer depth variability on the shelf in the northern Gulf of Alaska, 1974-1998. *Continental Shelf Research* 25: 2147-2162.
- Schroeder, F. and Koch, M. 2005. *Ferrybox Newsletter*. GKSS Research Center Institute for Coastal Research 6.
- Vodacek, A., Blough, N., DeGrandpre, M., Peltzer, E., and Nelson, R. 1997. Seasonal variation of CDOM and DOC in the Middle Atlantic Bight: Terrestrial inputs and photooxidation. *Limnology And Oceanography* 42: 674-686.
- Weingartner, T., Danielson, S. L., and Leech, D., 2010. GAK1 Time Series. [Available online from [http://www.ims.uaf.edu/gak1/.](http://www.ims.uaf.edu/gak1/)]
- Weingartner, T. J., Danielson, S. L., and Royer, T. C. 2005. Freshwater variability and predictability in the Alaska Coastal Current. *Deep-Sea Research II* 52: 169-191.
- WET Labs. 2003. *C-Star Transmissometer User's Guide Revision L*, WET Labs Inc., Philomath, OR.

WET Labs. 2004. ECO Fluorometer User's Guide Revision P, WET Labs Inc., Philomath, OR.

Zhang, Y., Wallace, J., and Battisti, D. 1997. ENSO-like interdecadal variability: 1900-93. *Journal of Climate* 10: 1004-1020.

### **Other References: Presentations**

Cokelet, E. D., 2008. *Tustumena* Ferrybox, invited talk given at the Alaska Marine Science Symposium special session entitled Shipboard Observing Systems: Using Instruments and Humans, a Roundtable Discussion, 22 January 2008, Anchorage, AK.

Cokelet, E. D., A.J. Jenkins, C.W. Mordy, W.S. Pegau, S. J. Baird and M.E. Sullivan. 2009. Long-term Oceanographic Measurements in the Alaskan Coastal Current from a Ferry, Alaska Marine Science Symposium, 19-22 January 2009, Anchorage, AK.

Cokelet, E. D., A.J. Jenkins, C.W. Mordy, W.S. Pegau and M.E. Sullivan. 2008. The Annual Cycle of Water Properties in the Alaska Coastal Current from Ferry Measurements, poster presented at the Alaska Marine Science Symposium, 20-23 January 2008, Anchorage, AK.

Cokelet, E. D., A. J. Jenkins, W. S. Pegau, C. W. Mordy and M. E. Sullivan. 2005. GEM Biophysical Observations Aboard an Alaska State Ferry, talk given at the Marine Science in Alaska 2005 Symposium, 24-26 Jan 2005, Anchorage, AK.

Cokelet, E. D., A. J. Jenkins, W. S. Pegau, C. W. Mordy and M. E. Sullivan. 2005. GEM Biophysical Observations Aboard an Alaska State Ferry, talk given at the NOAA/FOCI seminar series, 16 Feb 2005, Seattle, WA.

Cokelet, E. D., A. J. Jenkins, W. S. Pegau, C. W. Mordy and M. E. Sullivan. 2005. Biophysical Observations Aboard an Alaskan State Ferry, talk given at the ASLO Summer Meeting 2005, 19-24 June 2005, Santiago de Compostela, Spain.

Cokelet, E. D., A. J. Jenkins, W. S. Pegau, C. W. Mordy and M. E. Sullivan. 2005. Biophysical Observations Aboard an Alaskan State Ferry, talk given at the NOAA/NMFS/Auke Bay Lab., 16 Nov 2005, Juneau, AK.

Cokelet, E. D., A. J. Jenkins, W. S. Pegau, C. W. Mordy and M. E. Sullivan. 2006. GEM Biophysical Observations Aboard the Alaskan State Ferry *Tustumena*, poster presented at Alaska Marine Science Symposium, 23-25 Jan. 2006, Anchorage, AK.

Cokelet, E. D., A. J. Jenkins, W. S. Pegau, C. W. Mordy and M. E. Sullivan. 2007. Climate Shift and Ecosystem Differences Observed in Alaskan Ferry Oceanographic Measurements, poster presented at the Alaska Marine Science Symposium, 21-24 January 2007, Anchorage, AK.